Lawrence Berkeley Laboratory
UNIVERSITY OF CALIFORNIA
Physics Division

Invited talk presented at the Topical Conference,
Twelfth Annual SLAC Summer Institute on
Particle Physics, Stanford, CA, August 1-3, 1984

QUARK FRAGMENTATION IN e^+e^- COLLISIONS

P. Oddone

December 1984

Prepared for the U.S. Department of Energy under Contract DE-AC03-76SF00098

DISCLAIMER

QUARK FRAGMENTATION IN $e^+ e^-$ COLLISIONS ‡

P. Oddone
Lawrence Berkeley Laboratory
University of California
Berkeley, CA 94720

OUTLINE

I. INTRODUCTION AND COMMENT ON MODELS

II. PARTICLE PRODUCTION

Stable particles: π, K, p, Λ, Ξ, and resonances: ρ, ϕ, K^*.

III. PARTICLES IN EVENTS

a) Rapidity distributions relative to the event axis,

b) $p_\perp$ distributions relative to the event axis,

c) Three jet events: properties of the gluon jet (more baryons?),

particle flow as a function of particle type, energy-energy correlation.

IV. PARTICLE CORRELATIONS

a) Flavor correlations.

b) Baryon-baryon correlations.

V. CONCLUSION

---

‡ Invited talk presented at the Topical Conference, Twelfth Annual SLAC Summer Institute on Particle Physics, Stanford, California, August 1-3, 1984. This work was supported by the U.S. Department of Energy under contract number DE-AC03-76SF00098.

I. INTRODUCTION AND A COMMENT ON MODELS

In this brief review of new results in quark and gluon fragmentation observed in $e^+ e^-$ collisions, I have been quite selective; I shall concentrate mostly on PEP results and, within PEP, mostly on TPC results. The new PETRA results have been reported at this conference by M. Davier.[1] Given the organization of the topical conference I have restricted myself to results on light quark fragmentation since the results on heavy quark fragmentation have been reported by J. Chapman.[2]

In the study of fragmentation we try to understand how a state of initial partons at large Q^2 and small distances evolves in time and finally manifests itself in the laboratory as the usual mesons and baryons. We believe that quantum chromodynamics of quasi-free quarks and gluons is the correct dynamical description of the initial stages of the process.[3] The remnant of this few parton stage is observed in the laboratory as jets, ensembles of particles in which each particle has a small transverse momentum relative to the sum of momenta of the particles in the ensemble. While the initial observation of jets at SPEAR[4] was based on the statistical study of many events, jets observed at PEP and PETRA are dramatic and clear on an event by event basis. The first observation of hard gluon radiation as three jet events at PETRA[5] was conclusive after a handful of events. It is precisely the distinct nature of jets which makes the study of fragmentation interesting: to the extent the jets "remember" the original parton momentum they provide a means to test QCD calculations of the initial few parton stage; conversely, as we gain confidence in QCD calculations we can begin to explore models which evolve this initial state into the finally observed hadrons. The confinement mechanism which prevents the existence of free

quarks and gluons is not a well understood process. It is the inability to make rigorous calculations and predictions which has led to the creation of several phenomenological models which attempt to describe the data with relatively few parameters. Thus in the following paragraphs we compare the data with three phenomenological models: the independent fragmentation model (IF),[6] the Lund string model (LUND)[7] and the QCD cascade models of Webber[8] and Gottschalk.[9] These models are constantly evolving and have variants in the treatment of specific subprocesses (e.g. baryon formation). Thus LUND has evolved from "early LUND" to "standard LUND" to "symmetric LUND," the IF model has five or more variants depending on how the gluon is treated and how one implements energy and momentum conservation, and the QCD cluster models differ on how far the quark-gluon cascade is evolved before the formation of colorless clusters and on how the decay of clusters is matched to the existing data. With such multiplicity of models it becomes difficult to make definitive statements as to when such models fail in a fundamental way as opposed to failures which can be "fixed" without doing violence to the principles of the model. It is indeed a sign of progress that the new data allows us to make definitive statements regarding the failure of some models. The new data also provides a much higher level of detail which the models will have to attempt to fit or "explain."

Table I shows schematically some of the principal parameters of the models for the three families of models mentioned above. Typical parameters for the IF and LUND models are fragmentation functions, flavor suppression factors for the production of quark pairs, vector to pseudoscalar ratio for particle production, and additional parameters to describe baryon production which is handled in a variety of prescriptions. For the QCD cascade or cluster models the parameters are the QCD scale Λ, cut-off parameters for gluon radiation, mass parameters

TABLE I

Schematic description of the three models commonly used in this paper.

a) Independent fragmentation

Each quark, gluon fragments independently

f(z)=====>D(z)

Transv. mom. σ_q

V/P+V)

$u\bar{u} : d\bar{d} : s\bar{s} = a : b : c$

Gluon : your choice

Baryons: ad-hoc diquarks

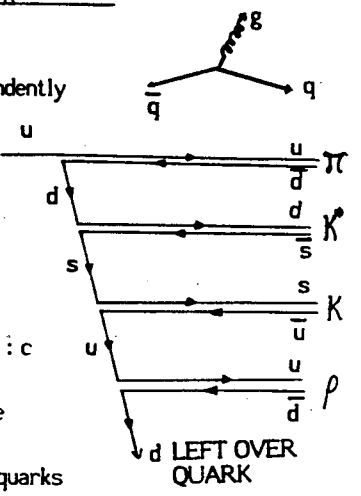

(Problem list: energy/momentum conservation, Lorentz invariance, left over quark matching....)

b.) Strings a la LUND

Opposite extreme: no independence

String tension: 16tons/m !

1GeV/fermi

$u\bar{u} : d\bar{d} : s\bar{s} : c\bar{c} =$
$1 : 1 : .3 : 10^{-11}$
Fixed by tunneling (m)

V/V+P

Fragmentation functs. a, b

Gluon ==> bent string
==> same formalism

Baryons: ad-hoc diquarks.

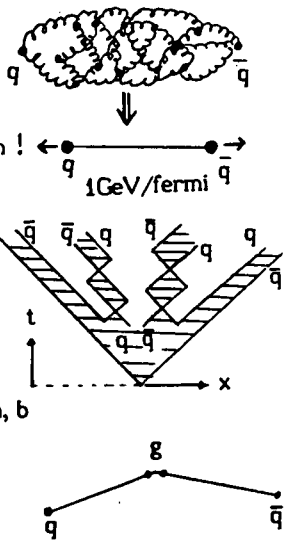

c) QCD Cascade -Cluster Models

Follow evolution using perturbative QCD to large number of partons (scale varies)

Form color singlet clusters in a pre-confinement stage

Produce hadrons by using parametrization of low energy data(particle data tables). YOU NEVER UNDERSTOOD THIS SOFT STUFF ANYWAY.

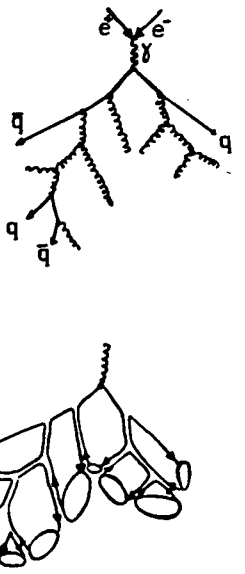

to control the mass scale of colorless clusters, and details on how the colorless clusters are matched to the existing low energy hadronic data. While these models are quite different from each other, they have been tuned sufficiently well to reproduce most of the features of the existing data. In instances where the models disagree with the data we shall remark whether or not such disagreement could stem at present from the lack of additional tuning.

II. PARTICLE PRODUCTION

Two new ingredients in the PEP program are the high resolution spectra provided by the HRS and the particle production measurements using the dE/dx identification of the TPC. In addition to the data from these two experiments, MkII and DELCO have made contributions in the measurement of resonance production. The number of measurements done in the last year is so large that a review in detail of each one is not possible in this short talk. I have summarized the measurements in Table II for mesons and in Table III for baryons. Asterisks in the upper left corner of each box indicate that the measurement has been reported in the last year. The number in the upper left corner of each box gives the reference number. For comparison the data from TASSO and JADE are also included in the tables. The impression that one derives from these tables is that gradually the production of stable particles and resonances is being well measured, with sufficient redundancy that the bad measurements and fluctuations are being found out. Particle production rates are the essential initial ingredients for all phenomenological models and it is not surprising that most models agree reasonably well with the measured ratios. One notable exception is the Gottschalk model which has a well known defect (at present) and predicts too few baryons.[10]

As examples of the progress made during last year I have selected some of the measurements and will describe them in brief detail. One interesting new measurement has been made by the HRS[11] using its superb momentum resolution ($dp/p^2 \simeq 0.1\%$, p in GeV) in the region $x = z \rightarrow 1$, where $x = 2 E_h/\sqrt{s}$ and s is the total center of mass energy. Here they have looked for the presence of a constant term in the differential cross section for charged particle production as expected by some models.[12] The differential cross section is shown in Figure 1. In the region of large x they find:

$$F(x) \propto (1-x)^2 + \mu^2/Q^2$$

where the 90% CL is $\mu < 4.4$ GeV/c.

Figure 2 illustrates the rapid progress in the measurement of ϕ production from the first measurements by TPC reported last summer[13] to the measurements reported by HRS this summer.[14] The LUND model prediction for ϕ production is also shown in the figure, and shows good agreement with the data.

Figure 3 illustrates the typically good agreement which the various experiments show when they measure the same process. The figure shows the differential cross section for Λ production as measured by MkII,[15] TASSO,[16] JADE[17] and TPC.[18] The LUND model prediction is shown superimposed on the data.

Figure 4 shows the differential cross section for K^+/K^-, $K^0/\bar{K}^0$, $K^{*0}/\bar{K}^{*0}$, and ϕ as measured by the TPC[19] together with the LUND model predictions. The cross sections for K^{*0} are not well reproduced by the present model

TABLE II: LIGHT MESON YIELD @ 29 --->34 GEV

Particle	MKII	TPC	HRS	DELCO	TASSO	JADE
ρ^0	★22 0.41 ±0.07 p>1 GeV		★33 0.58 ±0.06 x>.1		20 0.41 0.08 .1<x<.7	★24 0.98 ±0.17
K^{*o}	★22 0.35 ±0.09 p>1 GeV	★19 0.49 ±0.09	★33 0.36 ±0.06 x>.1	★25 large momenta		
$K^{*\pm}$	★22 0.29 ±0.10 p>2 GeV		★33 0.31 ±0.11 x>.1			★24 0.87 ±0.18
ϕ		★13 0.08 ±0.02	★14 0.08 ±0.01	★25 large momenta		
$K^{\pm}$	★26 small x only	★21 1.35 ±0.13			27 2.0 ±0.2	
K^o	★22 1.22 ±0.14	★19 1.22 ±0.15	★23 1.40 ±0.12		★28 1.60 ±0.1	★29 1.45 ±0.17
$\pi^{\pm}$		★21 10.7 ±0.6			27 10.3 ±0.4	
π^o		★30 5.3 ±0.6			31 6.1 ±2.0	
η						32 0.76 ±0.28

★≡NEW MEASUREMENT IN LAST YEAR. nn ≡REFERENCE NUMBER
SEE EXPLANATION OF NOMENCLATURE IN THE CAPTION OF TABLE III.

TABLE III: BARYON YIELD @ 29 ----> 34 GeV

The yield is shown as particles/event, where the error shown contains both the statistical and systematic errors (added in quadrature). The ★ in the left hand corner indicates the measurement is new in the last year. The number in the left hand corner shows the reference number. The yield is for the sum of particle and antiparticle.

Particle	MkII	TPC	HRS	TASSO	JADE
p		★21 0.60 ±0.08		27 0.80 ±0.10	17 small momenta
Λ	★15 0.21 ±0.03	★18 0.22 ± 0.02	★23 0.25 ±0.03	16 0.28 ±0.08	17 0.23 ±0.06
Ξ		★32 0.025 ±0.012		16 0.026 ±0.012	

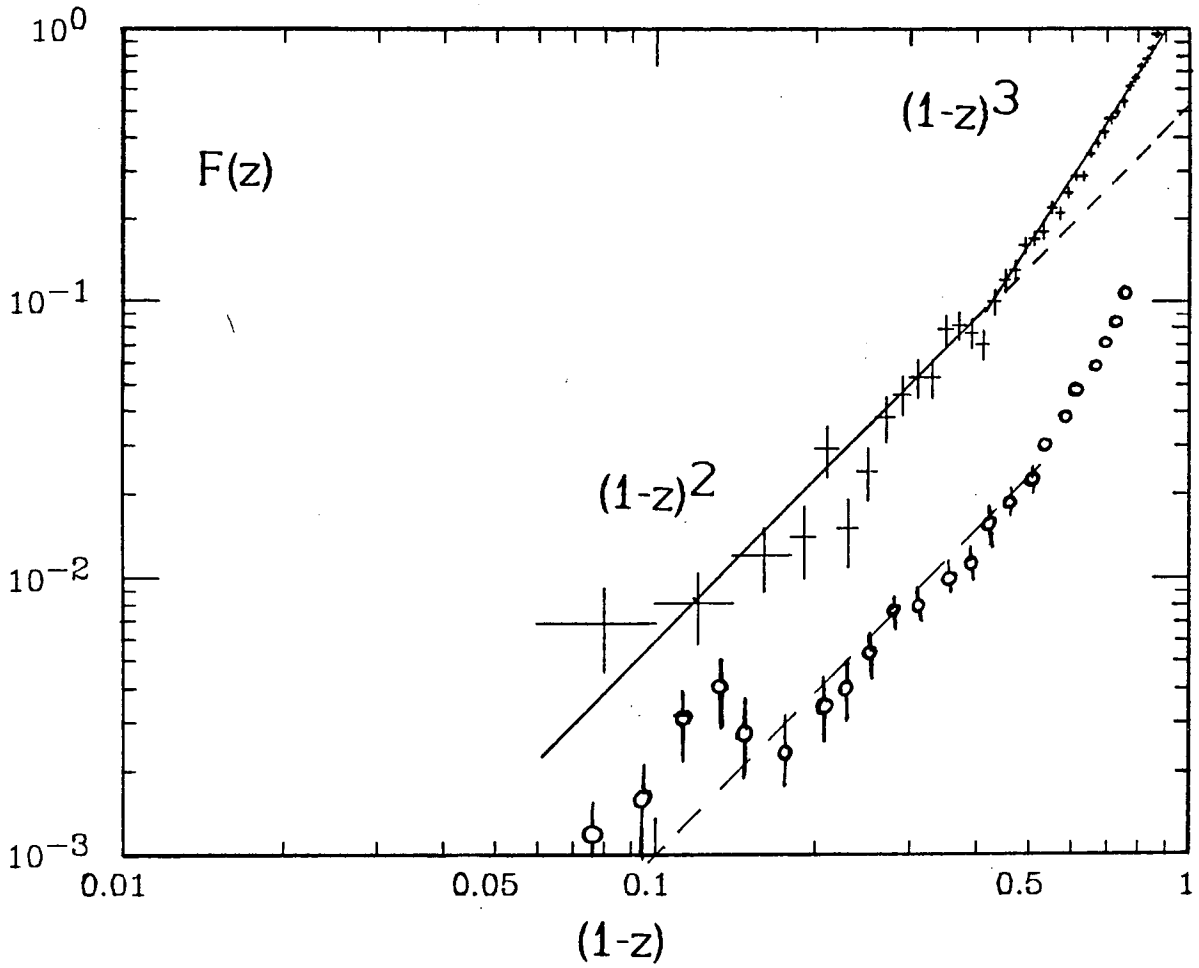

FIGURE 1

Invariant distribution $F(z) = (z/N_{ev})\ (dN^{had.}/dz)$ for charged particles measured by the HRS (crosses). The lower set of data points (circles) represents similar results for π^o production plotted a factor of five below the charged particle data.

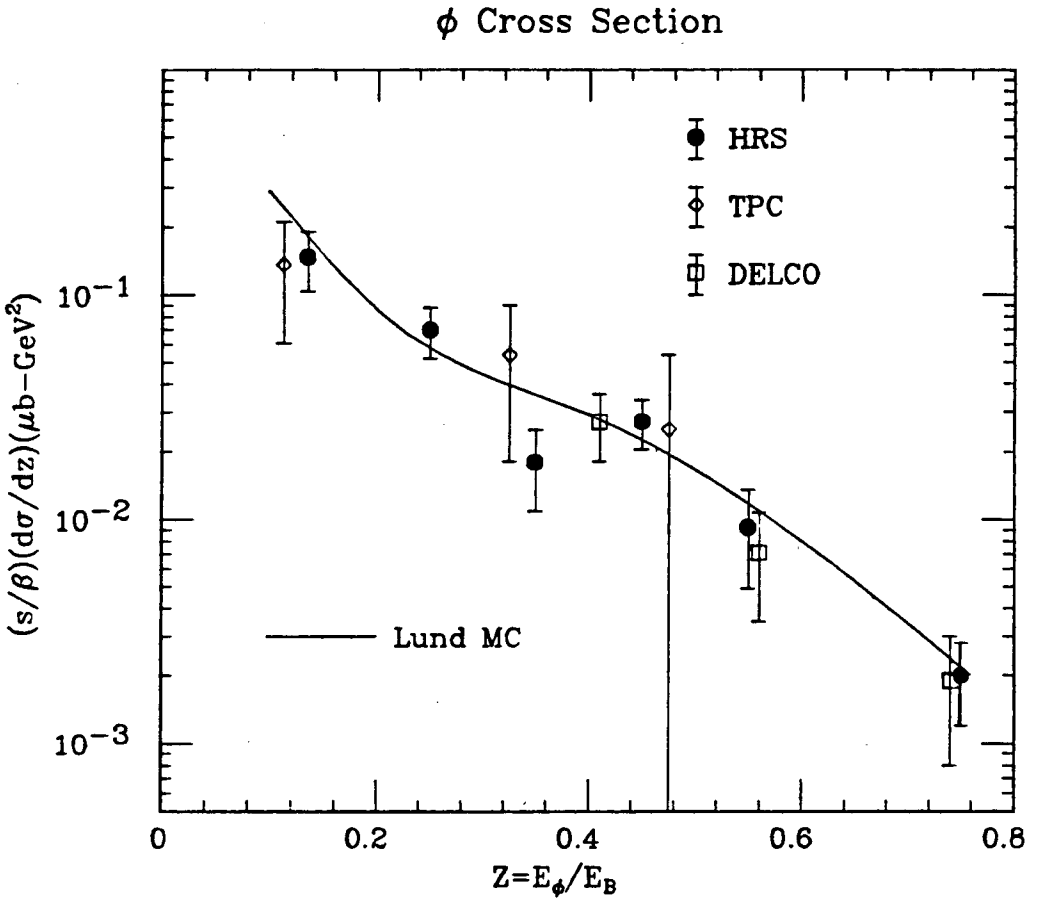

FIGURE 2

The ϕ inclusive differential cross section as a function of $z = E_\phi/E_{beam}$ as measured by the HRS, TPC and DELCO collaborations. See text for references.

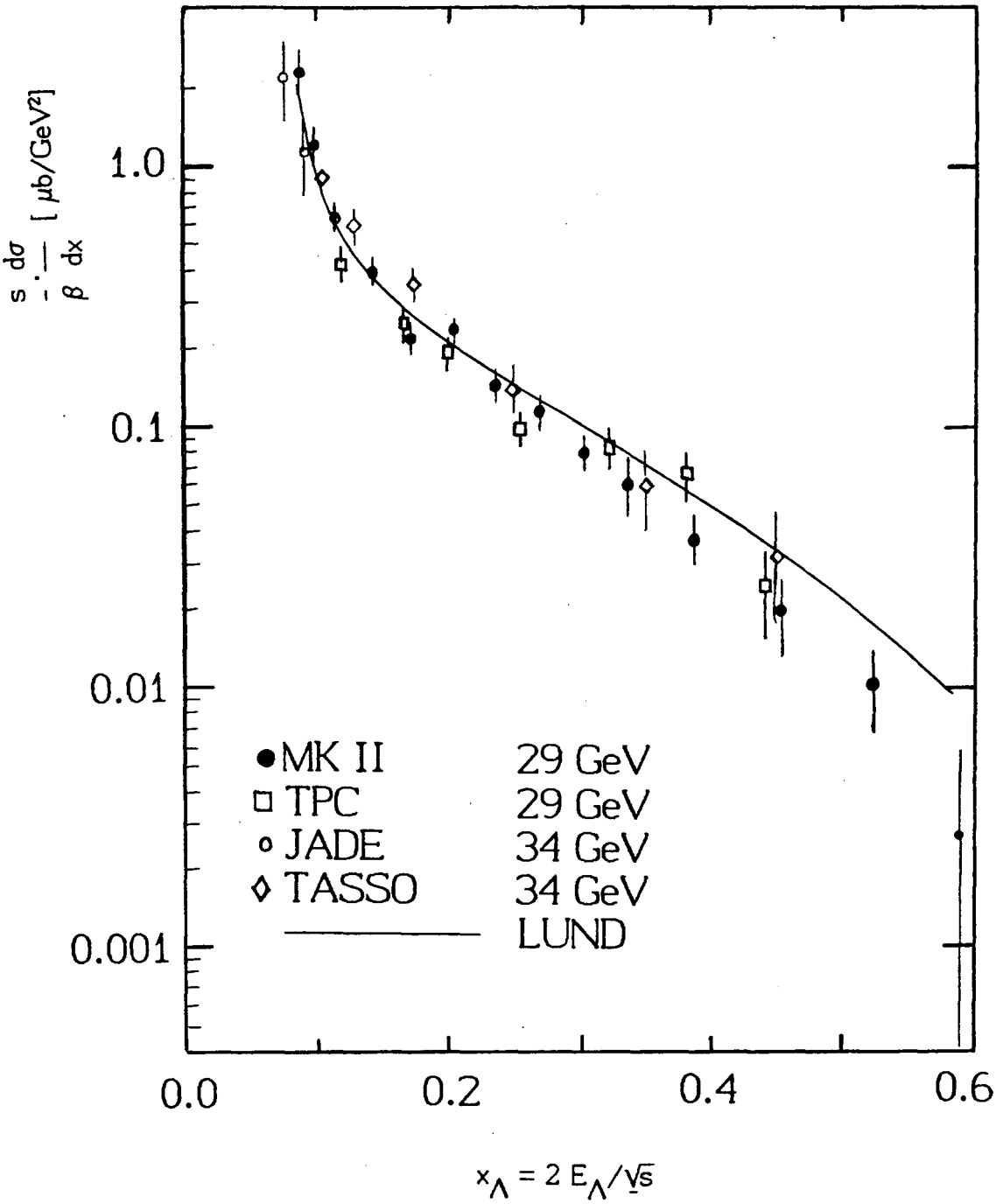

FIGURE 3

Inclusive Λ production as a function of $x = 2E_\Lambda/\sqrt{s}$ measured by the TPC, MKII, JADE and TASSO collaborations. See text for references.

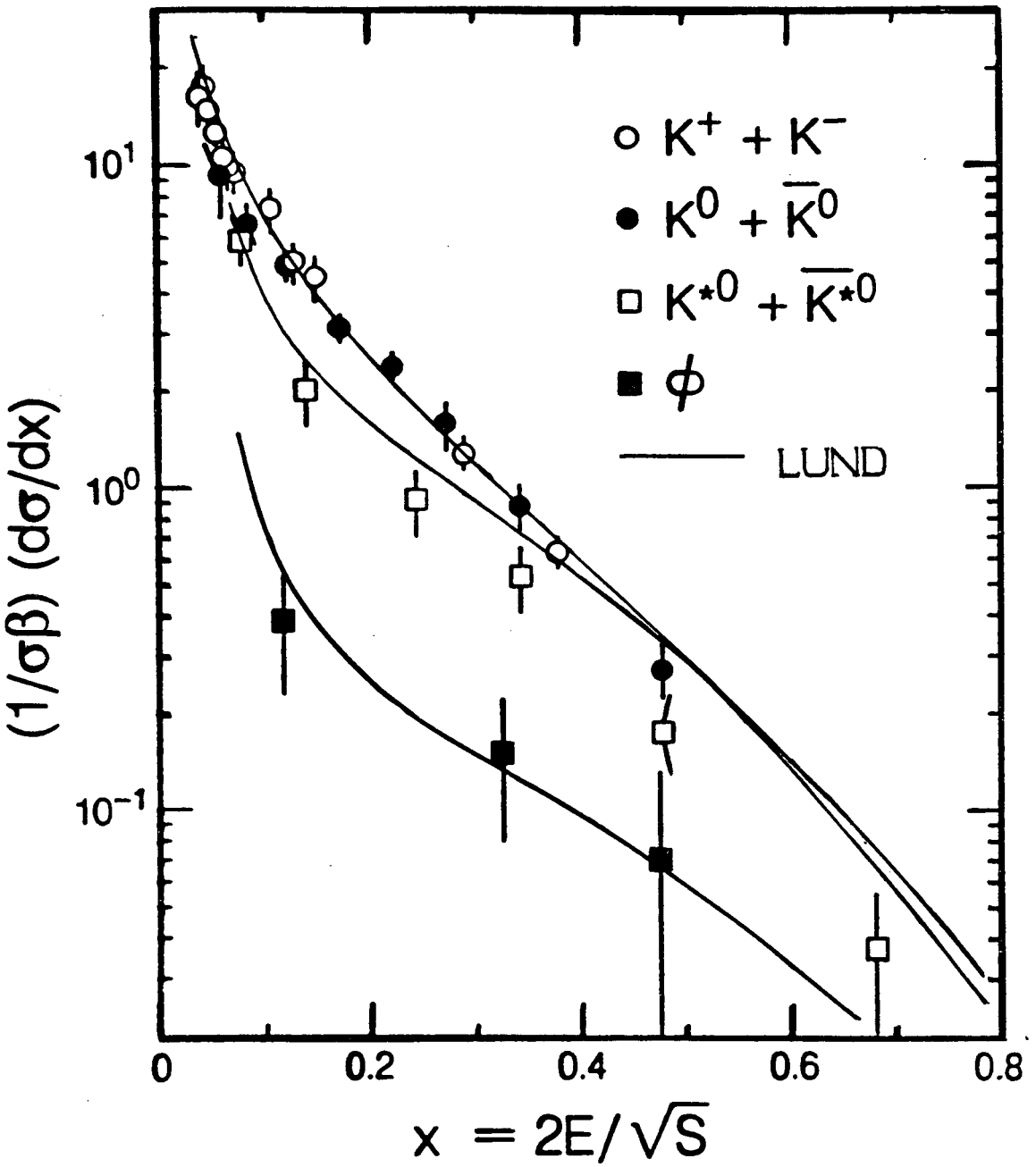

FIGURE 4

Differential cross sections vs. $x = 2E/\sqrt{s}$ measured by the TPC. For references see text and Table II. The solid lines are the LUND model calculations.

parameters, but no attempt to tune the model to this distribution has been made.

From measurements such as the ones described above and shown in Tables II and III many of the parameters which define the models can be obtained. For instance, the HRS[34] has made the observation that the ratio of π^o and ρ^o production for $x > .3$ is constant and independent of x. In this x region, given the flat ratio

$$\frac{(1/\sigma\beta)\ (d\sigma/dx)_{\rho^o}}{(1/\sigma\beta)\ (d\sigma/dx)_{\pi^o}} \simeq 1,$$

they argue that the observed π^o's cannot be feeddown from ρ^o's and thus a very direct measurement of the vector to pseudoscalar ratio can be made: V/V+P $\simeq$ 0.5 (no error analysis is yet available). The TPC[19] obtains the same ratio from K and K^* production as follows. First the number of particles per event are measured to be:

$$n(K^{*o}) = 0.49 \pm 0.04 \pm 0.07,$$
$$n(K^o) = 1.22 \pm 0.03 \pm 0.15,$$
$$n(K^{\pm}) = 1.35 \pm 0.13 \text{ (including systematics), and}$$

then the numbers are corrected for charm and bottom decays, where the ratio of D/D^* and B/B^* is set to 1/3 , and corrected for ϕ decays as measured in TPC to obtain:

$$n_c(K^{*o}) = 0.39 \pm 0.11,$$
$$n_c(K^o) = 0.82 \pm 0.16, \text{ and}$$

$$n_c(K\pm) \quad = 0.86 \pm 0.15.$$

With the further assumption that the number of $K^{\pm\star}$ is equal to $K^{o\star}$ we derive a ratio $V/(V+P)= 0.48 \pm 0.15$. This example illustrates that even after the measurement of particle production a considerable amount of gymnastics is involved in deriving a model parameter such as $V/(V+P)$. The error in the parameter depends on statistics and systematic errors of several measurements and on uncertainties in the decay branching ratios of charm and bottom resonances.

As a further example we can use the measured production fractions of ϕ's and $K^{o\star}$ to estimate the suppression factor for the production of $s\,\bar{s}$ pairs out of the vacuum. This ratio is

$$s/u = 2N(\phi)/N(K^{o\star}) = 0.37 \pm 0.15 \pm 0.8$$

after correction for charm and bottom decay. Using the measurement of ρ^o from TASSO[20] we further obtain

$$s/u = N(K^{o\star})/2N(\rho^o) = 0.32 \pm 0.09 \pm 0.05$$

indicating that a single parameter s/u appears to govern the $\phi/K^{o\star}$ and the $K^{o\star}/\rho^o$ production ratios as is assumed in many fragmentation models.

Much work remains to be done to obtain the best parametrization of the various models. Many distributions are now becoming available, not only for single particles but, as we shall see further on, for particle distributions in

relation to global event properties and in relation to other particles. We are beginning to do global fits to all available distributions. This work is in its early stages and no definitive numbers are yet available.

PARTICLES IN EVENTS

New data is now available on the production properties of different particles in relation to the event axis. These data are generally presented as rapidity distributions relative to the event axis and as transverse momentum distributions relative to the event axis. In addition it is possible to study particle production in events with three jets and thus be sensitive to differences between gluon and quark jets. In what follows we generally use the sphericity axis as the event axis unless explicitly stated otherwise.

A. Rapidity Distributions

TASSO[35] has studied rapidity distributions as a function of energy. As expected, with the standard definition of rapidity

$$y = 1/2 \ln \frac{E + p_L}{E - p_L},$$

the rapidity distributions show a plateau which broadens as a function of the energy. In addition a very shallow dip near zero rapidities was observed. New information is now available with separation of the different particle species π's, K's and p's. In particular, the small dip in the rapidity plateau near zero rapidity can be investigated as a function of particle type. This study is interesting because different models predict different behaviour near zero

rapidity, and in the cases where the same behaviour is predicted, it is predicted for seemingly very different reasons. The Webber cluster model predicts the dip as a consequence of soft gluon interference, or equivalently, ordering of gluon emission angles. The Gottschalk model predicts a dip due to the presence of relatively large mass clusters which move away from each other and tend to deplete the region near zero rapidity. The LUND string model predicts a dip because in three jet events there are in effect two strings which fragment independently while they move away from each other depleting the region near zero rapidity. The IF model predicts no dip in its usual variants. It is also possible to ascertain whether or not the dip near zero rapidity is an artifact of having assigned the pion mass to all particles in previous studies.

Figure 5 shows the contribution of the various particle species to the rapidity distribution when they all are called π's. It is evident from the figure that the dip exists for pions as well as for other species and that it is somewhat accentuated when all particle species are added together. Figures 6 through 8 show the rapidity distributions for the different species when they are correctly identified. Three curves are superimposed on the data: the LUND model, the cluster model of Webber and the cluster model of Gottschalk. The conclusions that we can draw from these graphs are:

1. The data show significant dips near $y \simeq 0$ for both π's and K's, but no significant dip, albeit with poorer statistics, for p's.

2. Qualitatively both the LUND string model and the QCD cluster models get dips near $y \simeq 0$. The detailed agreement between the models and the data is, however, comparatively poor. In particular, for π's the LUND model gets too shallow a

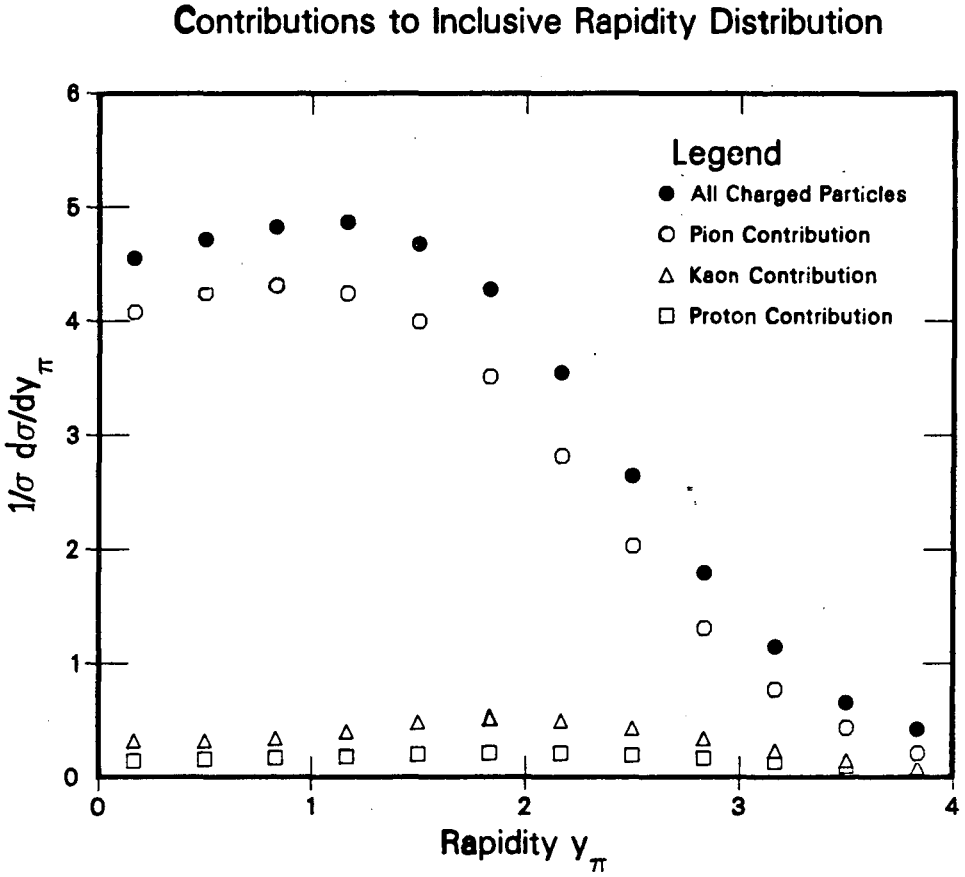

FIGURE 5

Contributions to the inclusive rapidity distribution of charged particles when all charged particles, π's, K's and p's, are assumed to be π's.

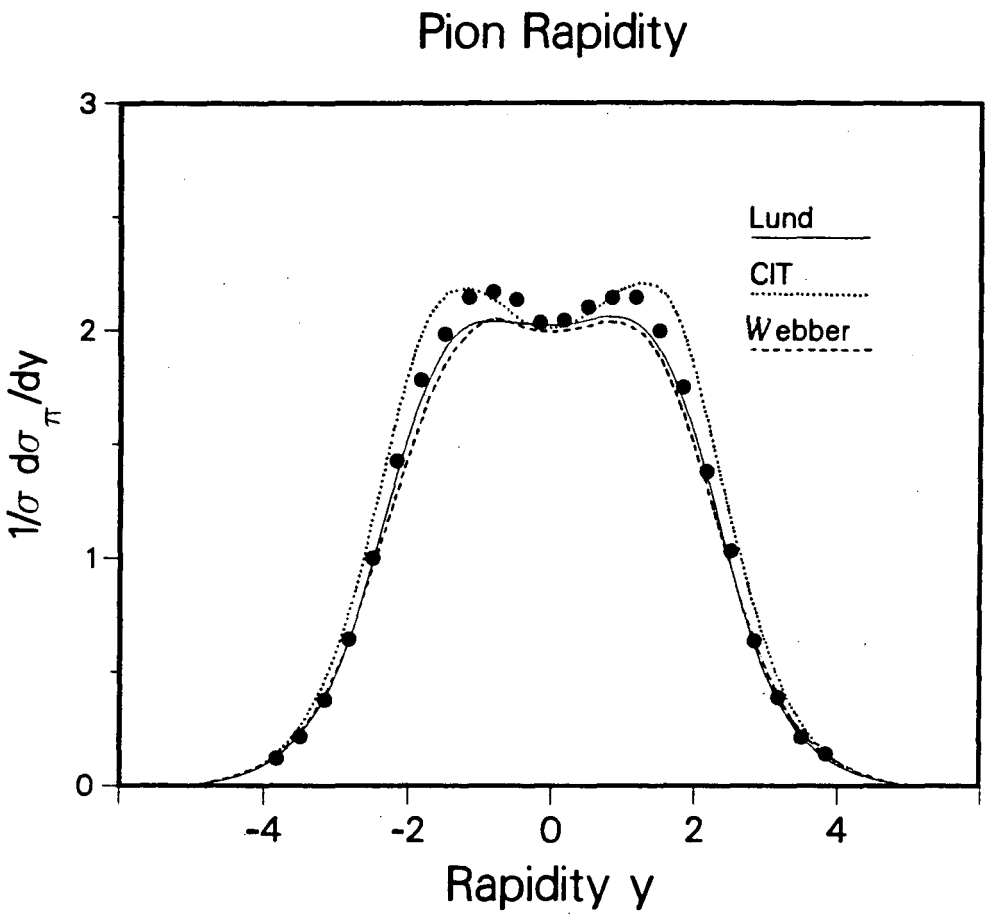

FIGURE 6

Pion inclusive rapidity distribution for identified pions measured by the TPC.

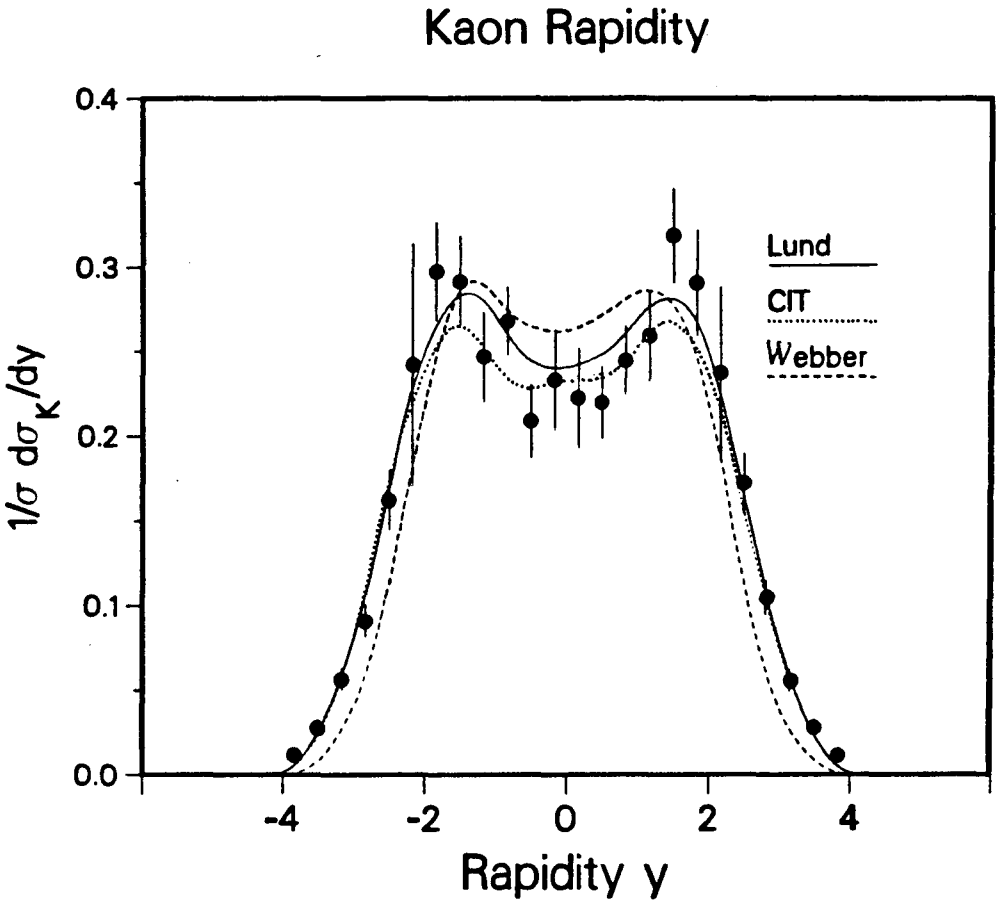

FIGURE 7

Kaon inclusive rapidity distribution for identified kaons measured by the TPC.

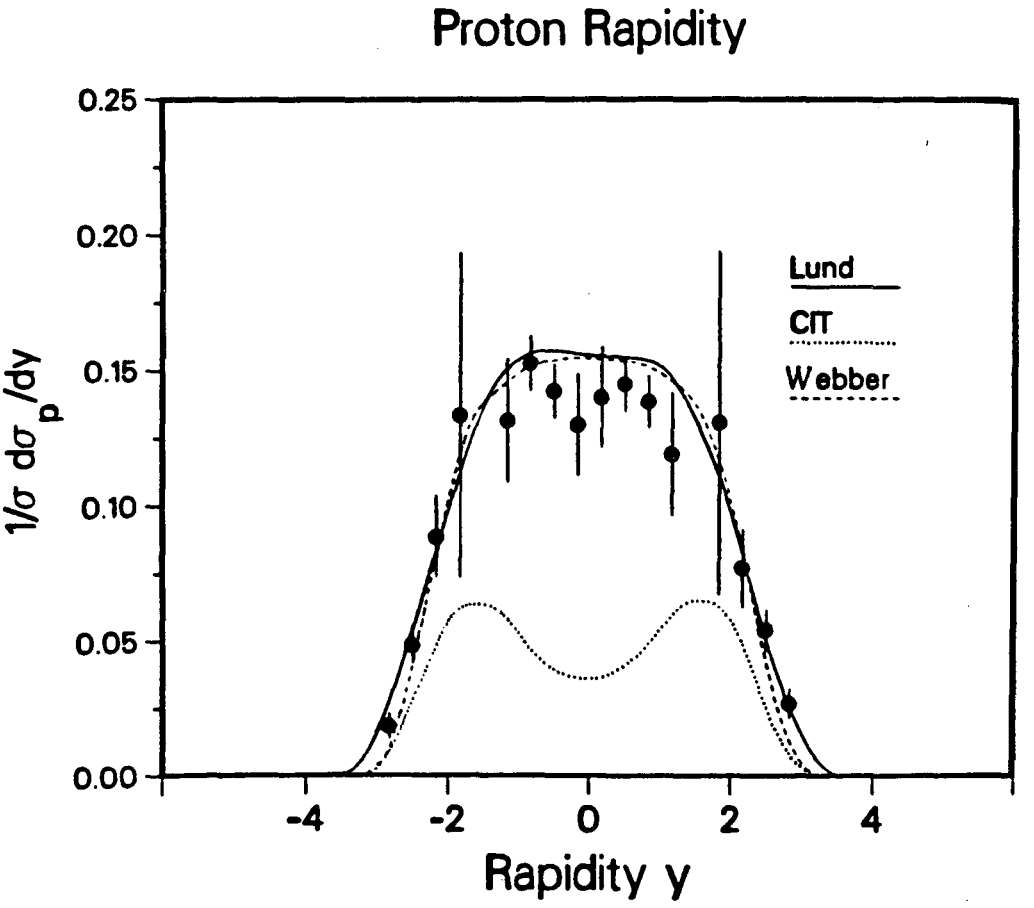

FIGURE 8

Proton inclusive rapidity distribution for identified protons measured by the TPC.

dip, a feature which is also present in the QCD models. In addition, the Webber model has too narrow a rapidity distribution for K's, and the Gottschalk model is poorly tuned and has too few baryons (well known problems of the present versions, which can presumably be fixed).

It is too early to tell whether the quantitative diagreement between the data and the models is fundamental or fixable by more tuning of the models. As we will see in the following sections relatively small effects can be very significant and can rule out some models.

B. Transverse Momentum

The experimental observation regarding transverse momentum distributions relative to the sphericity axis is quite unambiguous: heavier particles such as Λ's, p's, or resonances such as the ϕ's show a considerably higher transverse momentum relative to the event axis. This is illustrated in Figure 9 which shows the transverse momentum distribution of ϕ's and of π's measured in the TPC.[13] Similarly Figure 10 shows the transverse momentum distribution of Λ's measured by the MkII[15] compared to all charged particles measured by the MkII and to pions measured by the TPC.[21] It is interesting that essentially all models have no problems fitting the transverse momentum distribution of all the observed particles. Generally all primary mesons have the same transverse momentum distribution and all primary baryons have the same transverse momentum distribution (which can be different from the meson distribution). The differences in transverse momentum distributions of observed particles are due to resonance decay: a) more of the heavy resonances such as ϕ's are primary and have a stiffer spectrum closer to the primary distribution, and b) heavy

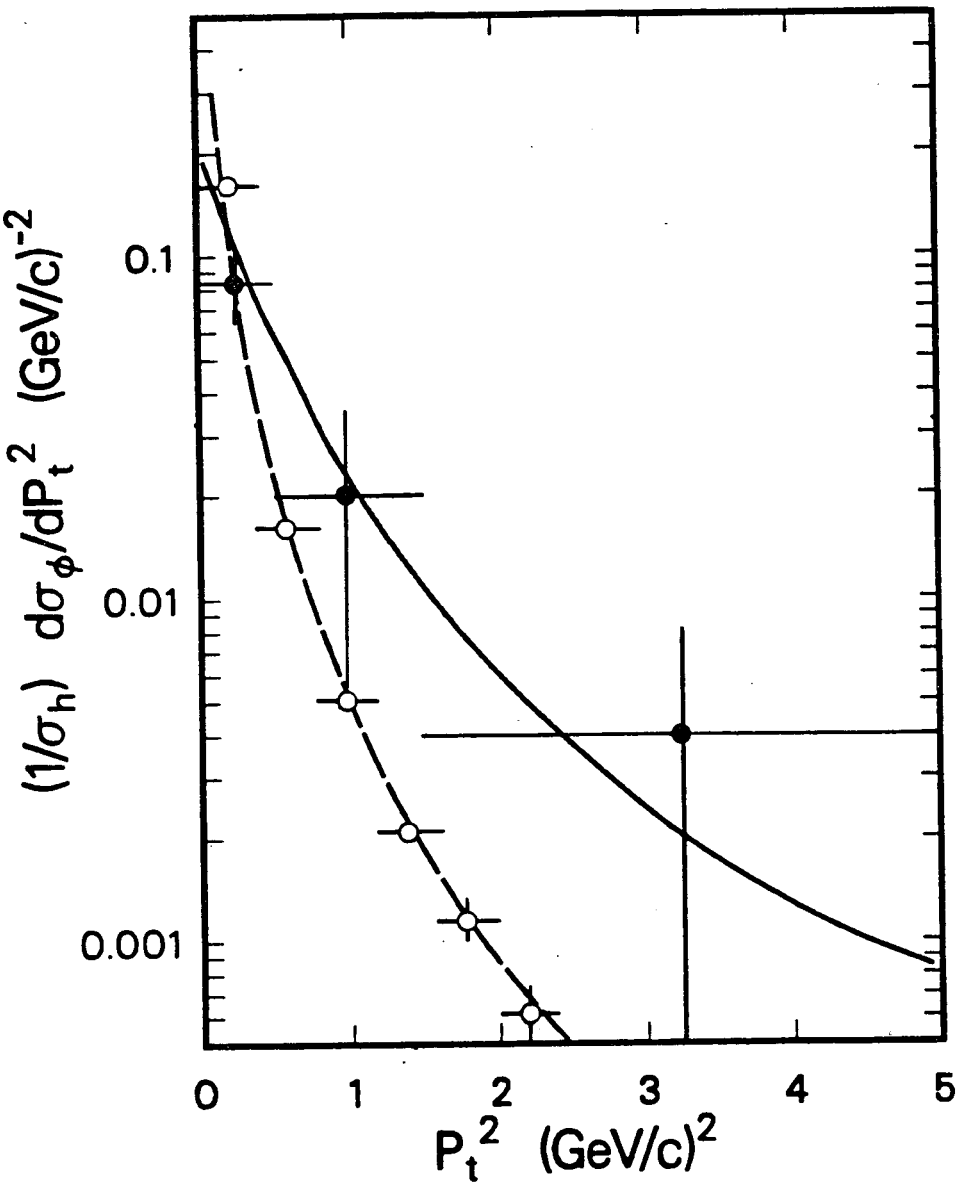

FIGURE 9

Distribution of the square of the ϕ transverse momentum with respect to the thrust axis in the range $x_\phi < 0.55$ (indicated by filled circles). The open circles give the distribution observed for $\pi^\pm$ scaled by 1/140. The solid and dashed lines show the predictions of the LUND model. The data is from the TPC.

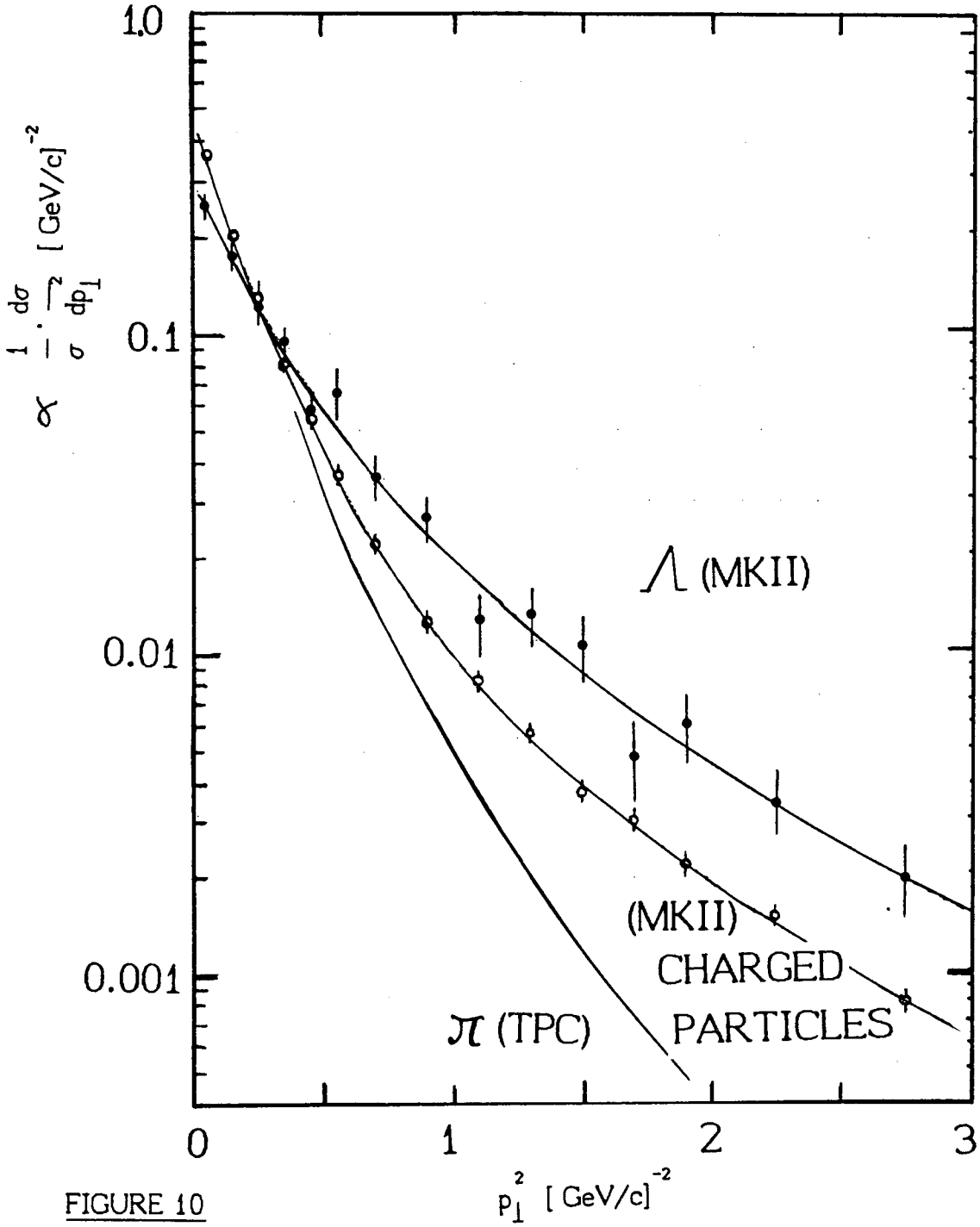

FIGURE 10

Transverse momentum distribution relative to the thrust axis for Λ's (upper curve) and all charged particles (middle curve), both measured by the MKII, compared to π's measured by the TPC (lower curve).

particles carry most of the momentum in the decay of resonances and therefore have a transverse momentum closer to the primary particles.

In particular, because the spectra of baryons are more sensitive to the primary spectrum, it is possible to investigate the mechanisms of baryon formation by studying the transverse momentum distribution of baryons.[36] Figure 11 shows the transverse momentum distribution for protons measured in the central rapidity plateau in comparison with two model predictions based on the LUND Monte Carlo. In one model the baryon is formed by three independent quarks ($p_\perp = \sqrt{3}\, p_{o\perp}$) and in the other the baryon is formed by a quark and a diquark ($p_\perp = \sqrt{2}\, p_{o\perp}$). The data seems to favor the second model with baryons being formed by a quark and a diquark.

C. Three Jet Events

More baryons in gluon jets? Yes, but.....

One question which can be answered with the data available from the TPC[36] is whether or not there are more baryons in gluon jets. To investigate this question we compare the particle fractions in events with gluon radiation (sphericity greater than 0.3) and two jet events (sphericity less than 0.15). Figure 12 shows this comparison for protons as a function of the proton momentum. It is evident from the figure that three jet events have enhanced proton production for large momentum protons. . On the other hand, the LUND model also shows this enhanced proton production without making any assumptions about a gluon jet having more baryons. In fact, in the LUND model, three jet events correspond to fragmentation of two strings which are essentially the same strings as are

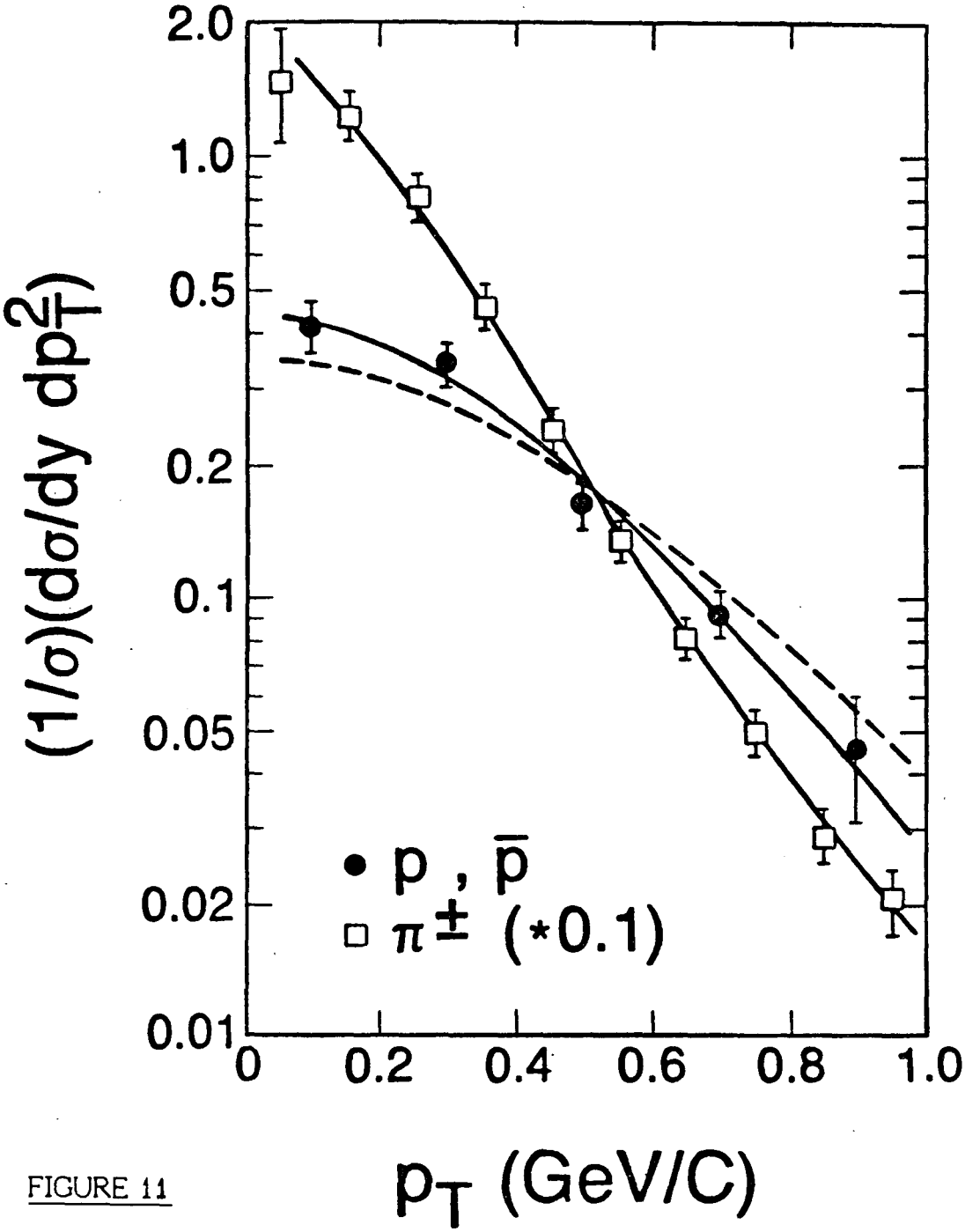

FIGURE 11

The $p_\perp$ dependence of proton and pion cross sections for rapidities $|y| < 1$. The full lines are the predictions of the LUND model (proton production via di-quarks) and the dashed line is the prediction for proton production via recombination of three individual quarks. The data is from the TPC

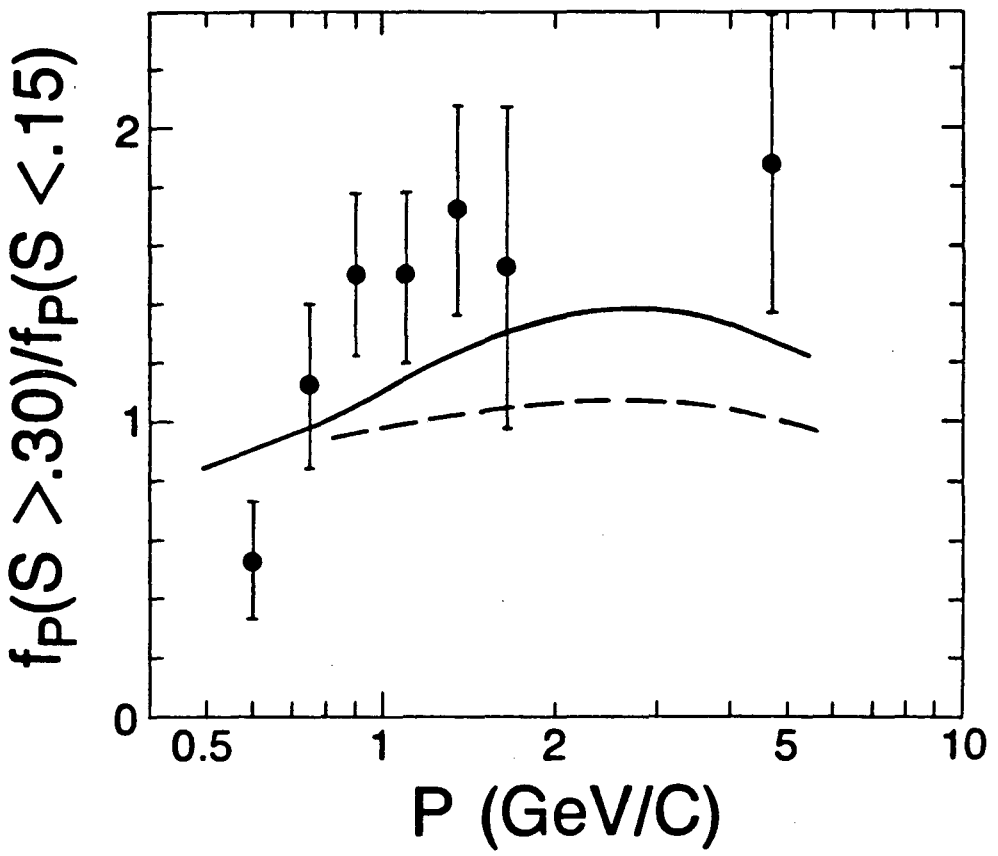

FIGURE 12

The ratio of proton fractions in events with high (>.3) and low (<.15) sphericity, as a function of momentum. Full and dashed lines show the predictions of the LUND model for final state hadrons and primary hadrons respectively. The data is from the TPC.

present in two jet events. Furthermore, the ratio of primary baryon production for events of high and low sphericity is approximately flat and equal to 1 in the model. The enhanced proton production predicted by the model exists only after resonance decay as is shown by the solid line in Figure 12. Thus purely kinematical effects are able to account for the enhanced proton production without invoking a different mechanism for proton production in gluon fragmentation.

Particle flow in three jet events: A test of models

One important question which differentiates models is whether or not the observed hadrons originate from sources which are Lorentz-boosted relative to the overall center of mass system. JADE[37,38] has reported that particle flow in three jet events favors the IF model over the LUND model. TPC has now confirmed this effect and extended the study to additional models,[39,40] using better particle identification.

In IF models, each parton fragments into a jet of hadrons independently. Thus in three jet events the regions between the jets are populated by the same mechanism: the momentum distribution transverse to the jet axes (Figure 13a).

In the LUND model three jet events are represented by a string that stretches from the quark to the gluon and then to the antiquark (Figure 13b). The two string segments fragment in their respective rest frames. Hadrons thus receive a Lorentz boost as observed in the overall center of mass system. As a result the distribution of hadrons in the regions between the jets is altered: the region qg and the region $\bar{q}g$ are favored by the boost, while the region $q\bar{q}$ is comparatively

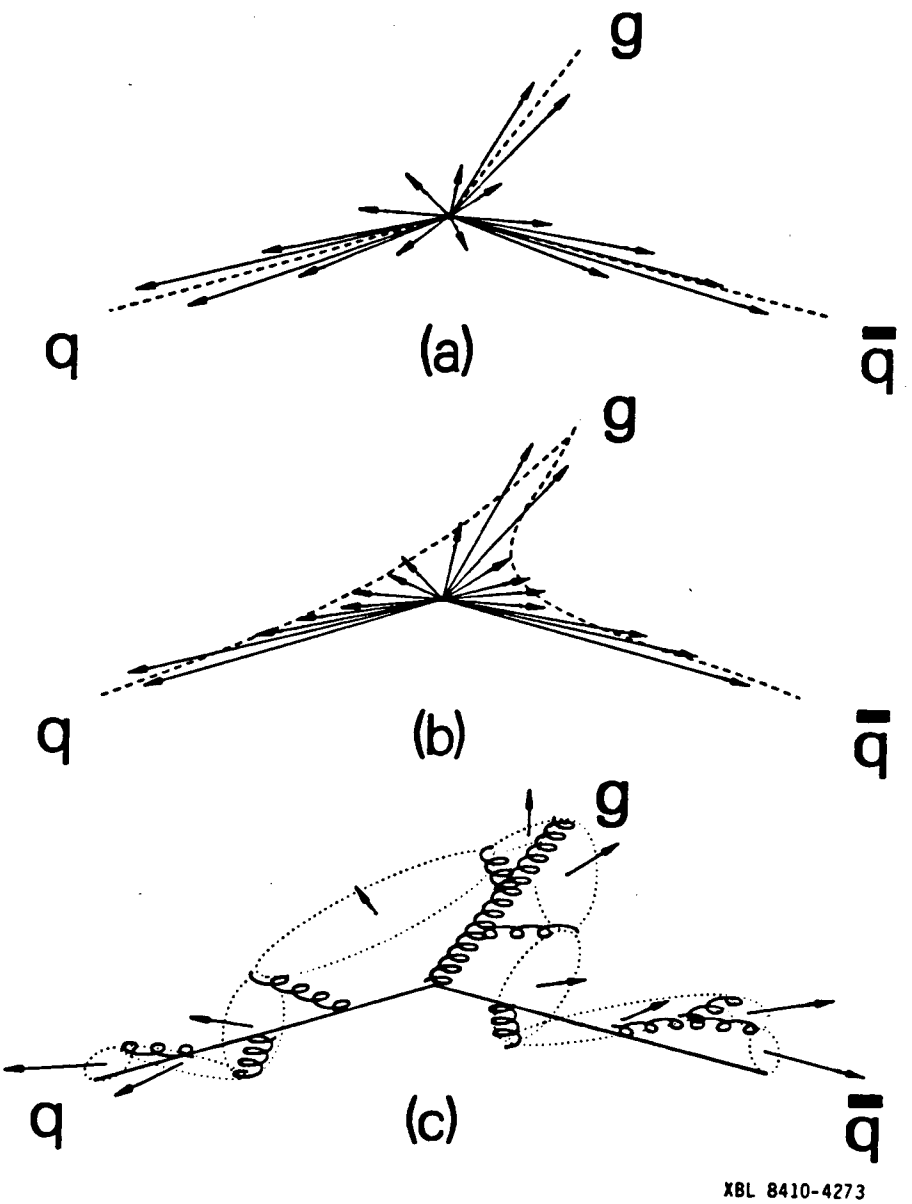

FIGURE 13

The 3-jet event structure for the (a) IF, (b) LUND, and (c) Cluster models. The arrows in (a) and (b) indicate the momentum space distribution of particles. The dashed lines in (a) represent the parton directions, in (b) the strings. (c) shows the quark-gluon cascade (solid and curly lines) and the clusters (dotted ellipses).

depleted.

In the Webber cluster model the initial partons initiate a quark-gluon cascade described by leading-log QCD. Soft gluon interference is included leading to angle ordering in the cascade: successive parton emission angles are smaller than the preceeding ones. Since the angle between the q and $\bar{q}$ is usually large, this ordering causes the formation of clusters to preferentially populate the qg and $\bar{q}g$ regions rather than the $q\bar{q}$ region. The decay of the moving clusters then produces a "boost signal" similar to that of the LUND model. Not all cluster models predict the same behaviour. For instance, the Gottschalk model which does not have angle ordering in the quark-gluon cascades does not predict the depopulation of the $q\bar{q}$ region relative to the qg and $\bar{q}g$ regions.[40]

Approximately 10% of the 29000 events used in the TPC analysis are classified as three jet events using fairly standard jet finding algorithms. The jets are labeled 1, 2, and 3 such that jet 1 is opposite the smallest angle between jets, and jet 3 is opposite the largest angle. The angle ϕ is defined in the event plane and proceeds from jet 1 ($\phi = 0^0$) to jet 2 ($\phi \simeq 155^0$) to jet 3 ($\phi \simeq 230^0$) and back to jet 1 ($\phi = 360^0$).

Figure 14 shows the normalized particle density $(1/N)dN/d\phi$ along with the predictions of the three models described above (IF, LUND and Webber) for all charged particles and photons (14a), for particles with large momentum out of the event plane (14b) and for heavy particles (14c). The highest particle density occurs in the jet 1 peak and the lowest in the jet 1-2 valley. The LUND model provides a reasonable description of the data over the entire ϕ range. The IF model provides nearly as good a description, except in the jet 1-2 valley

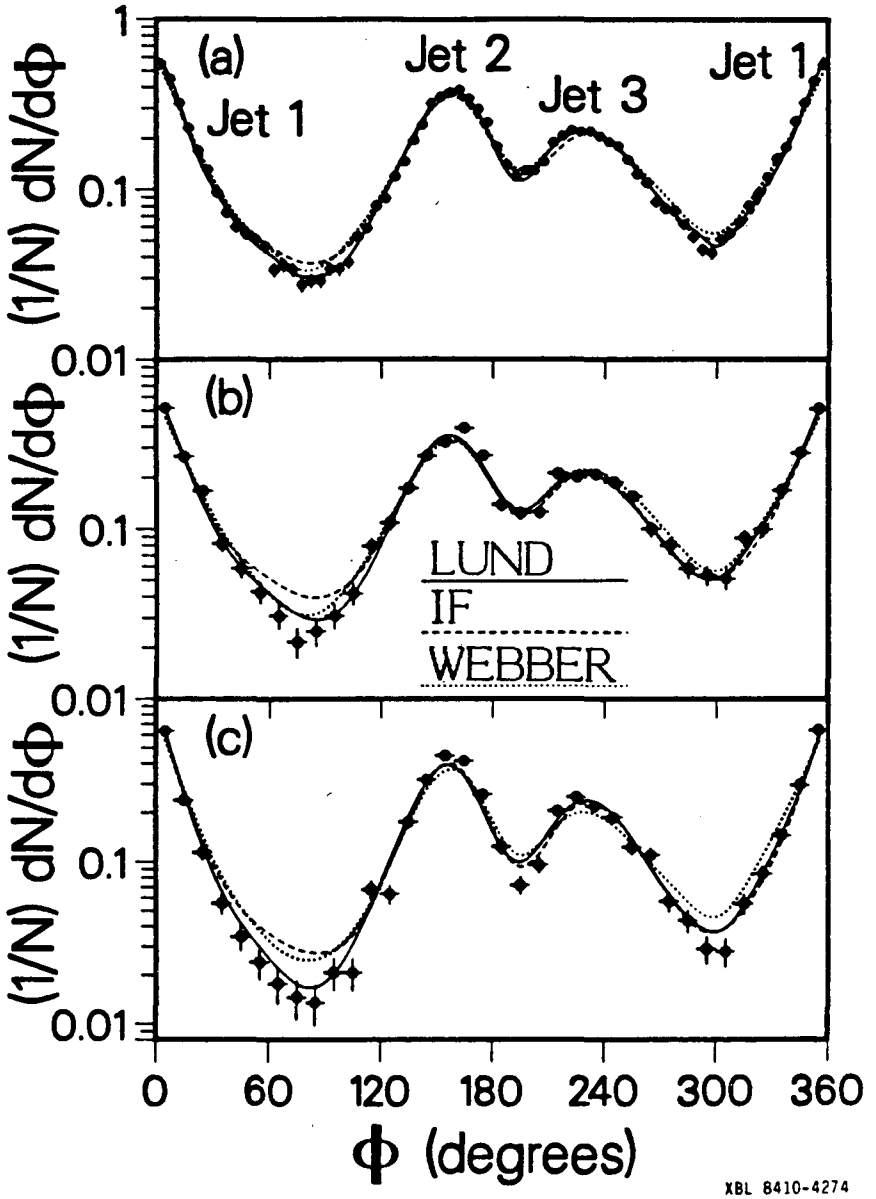

FIGURE 14

Particle density $(1/N)dN/d\phi$ in 3-jet events for (a) all charged particles and photons, (b) those charged particles and photons satisfying $0.3 < p_{out} < 0.5$ GeV, where p_{out} is the momentum out of the event plane, and (c) a heavy particle sample of charged and neutral K's, p's and Λ's. Also shown are the predictions of the IF, LUND and Webber cluster models. The data is from the TPC.

where it predicts a density 30% higher than the data. As expected from the nature of the Lorentz boost, the effects are accentuated for particles with large transverse mass $m_\perp = \sqrt{m^2 + p_\perp^2}$. Thus the discrepancy with the IF model increases to a factor of 2 for either particles with large momentum relative to the event plane or for particles with large mass. The discrepancy is fundamental and cannot be "patched-up" in the present variants of the IF model: the IF model cannot be tuned to fit the 1-2 valley and provide reasonable fits of global event distributions. For the Webber model the predictions are too large for all regions between jets; this result is sensitive to model parameters which have not been tuned for this particular analysis.

A quantitative summary can be made by studying the "normalized particle populations " N_{ij}. For each particle between jets i and j the angle between the jet i and the particle is divided by the angle between jets i and j. N_{ij} is the number of particles between .3 and .7 in this normalized angular region (the most sensitive to boost effects). The comparison of the jet 1-2 region and the jet 1-3 region is made by the ratio N_{31}/N_{12}. This ratio is insensitive to the variants of the IF model, to tuning of the Webber model and to detector acceptance. For IF models we expect $N_{31}/N_{12} \simeq 1$ independent of particle mass or transverse momentum out of the plane, while for boosted hadron sources in the LUND and Webber models we expect the ratio to be greater than 1 and to increase with mass and momentum out of the plane.

The ratio N_{31}/N_{12} is shown in Figure 15. The data show that the ratio increases with mass and with momentum out of the plane. The LUND and the Webber models give a good description of the behaviour of this ratio, while the IF model does not fit the data.

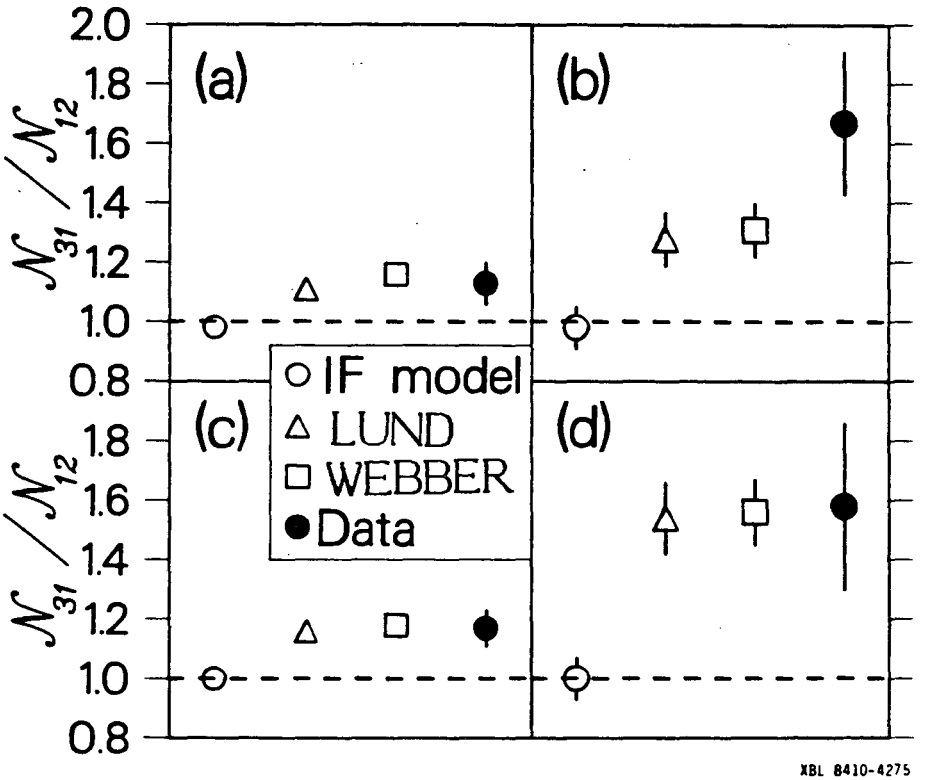

FIGURE 15

The ratio N_{31}/N_{12} of the populations between jets, for the data and the models: (a) shows the ratio for pions with $p_{out} < 0.2$ GeV, and (b) shows the ratio for pions in the range $0.3 < p_{out} < 0.5$ GeV, (c) shows the ratio for all pions and (d) for the heavy particle sample. The data is from the TPC.

Energy-energy correlations

Additional evidence against the IF model has been provided by MAC with the study of energy-energy correlations [41] The MAC group has shown that the energy-energy correlation is fit well by the LUND model while it is fit poorly by the variants of the IF model. It is interesting to note that the values of α_s obtained by MAC from the study of energy-energy correlations and by TPC in the study of global distributions[39],[40] are remarkably close when they use a model that fits the data such as the LUND model

$$\text{MAC} \quad \alpha_s \, (LUND) = 0.185 \pm 0.013 \, , \text{ and}$$
$$\text{TPC} \quad \alpha_s \, (LUND) = 0.183 \pm 0.010.$$

The conclusions from either the particle flow analysis of TPC and JADE, or the energy-energy correlations of MAC, tend to rule out the Independent Fragmentation model in its presently known variants. The LUND model fits the data well. The QCD cluster model of Webber is not as close to all aspects of the data as the LUND model but on the other hand it has not been as extensively tuned as the LUND model.

IV. PARTICLE CORRELATIONS

A. Flavor Correlations

From the TPC we now have $\pi\pi$, πK, and KK rapidity correlations.[42] Since the primary quarks in the annihilation event carry opposite quantum numbers and occupy regions of phase space which are vastly separated, we expect to observe long range correlations (LRCs) reflecting the initial separation of quantum

numbers. On the other hand, the final formation of hadrons is a small Q^2 phenomenon which we expect will generate short range correlations (SRC's). Figure 16 illustrates the mechanisms for LRC's and SRC's in the case of (a) pions arising from primary light quarks and (b) pions and kaons arising from heavy quarks.

With the usual definition of rapidity (see discussion of rapidity distributions above) we can define the flavor tagged charge density $q_a^b(y)$ as the net compensating charge density seen in particles of species b when the test particle is of species a:

$$q_a^b(y) = \rho_b^{opposite\ a}(y) - \rho_b^{same\ a}(y)$$

where the superscripts *opposite* (*same*) a indicate particles of species b with the opposite (same) charge as a. When calculating $q_a^b(y)$ the data must be corrected for sample purity and detection efficiency by unfolding the measured two particle π, K and p combinations using Monte Carlo determined misidentification probabilities and acceptances.

Figures 17a and 17b show the $\pi\pi$ rapidity correlations with results similar to the charge compensation results previously observed in e^+e^-[43] and pp[44] collisions. When the test π is chosen at small rapidity y_{test} the dominant feature is SRC's due to resonance decay and presumably local charge compensation in the hadronization process. For large y_{test} LRC's become evident and provide evidence for charged primary partons.

Figure 18a shows KK correlations for large y_{test}. The LRC is now

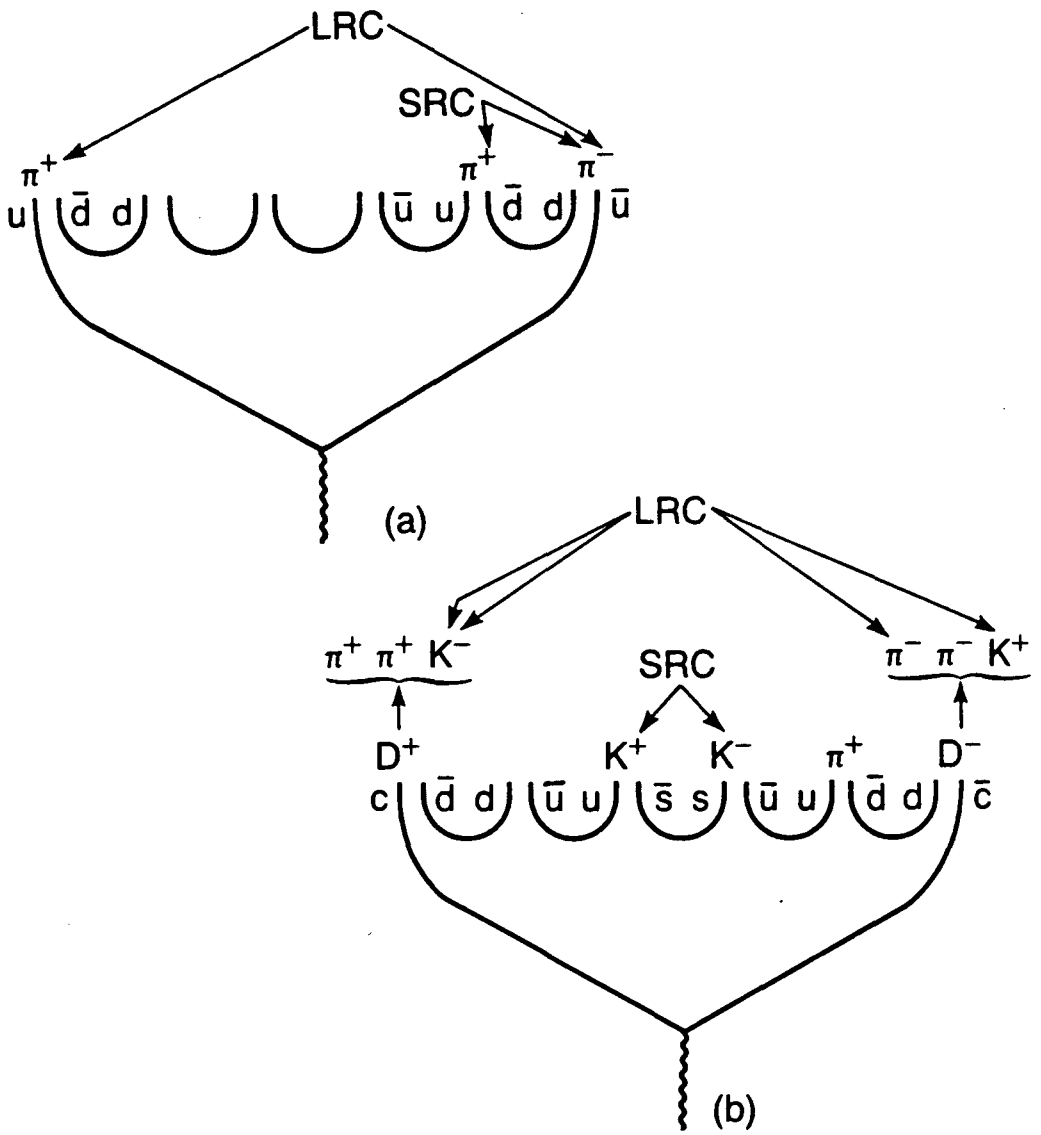

FIGURE 16

The mechanisms responsible for long- and short-range flavor correlations (a) among pions and (b) between pions and kaons.

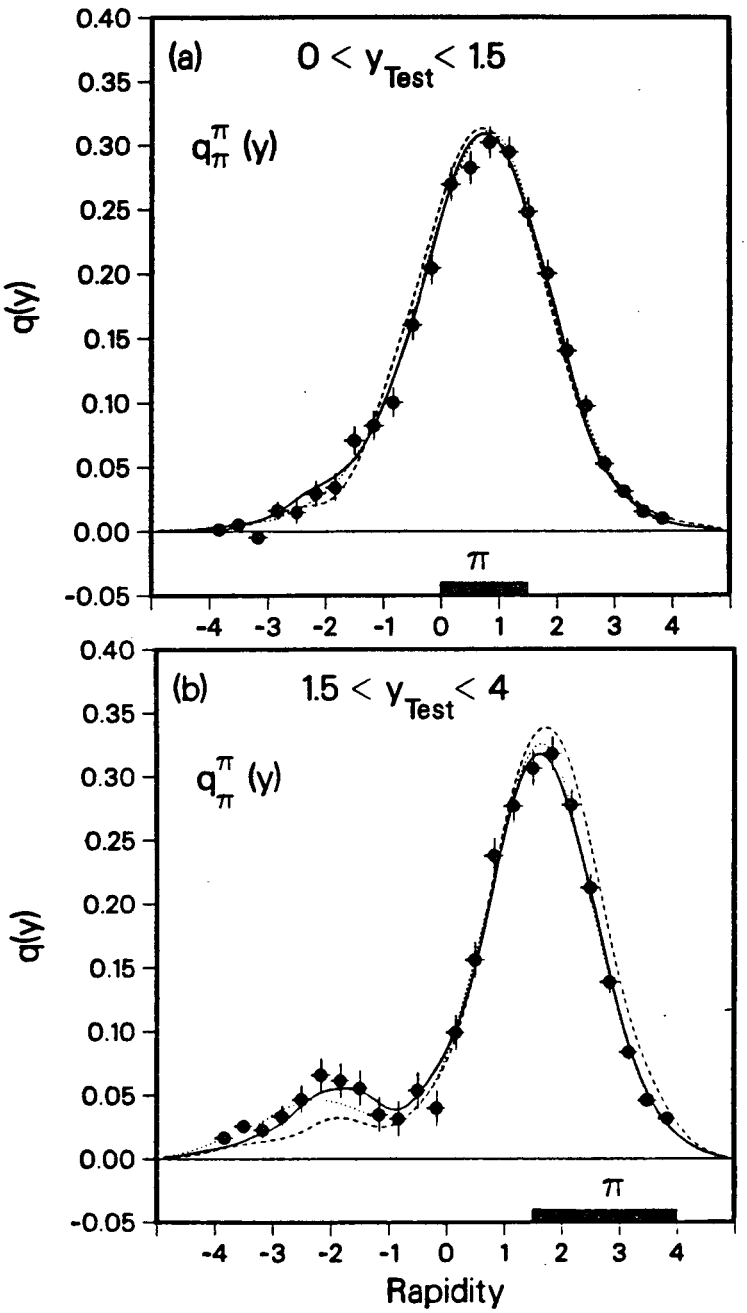

FIGURE 17

The $\pi\pi$ associated charged density for two different rapidity intervals. The solid and dotted lines give the predictions of the LUND and Webber models. The dashed line is the LUND model without heavy quarks. The data is from the TPC.

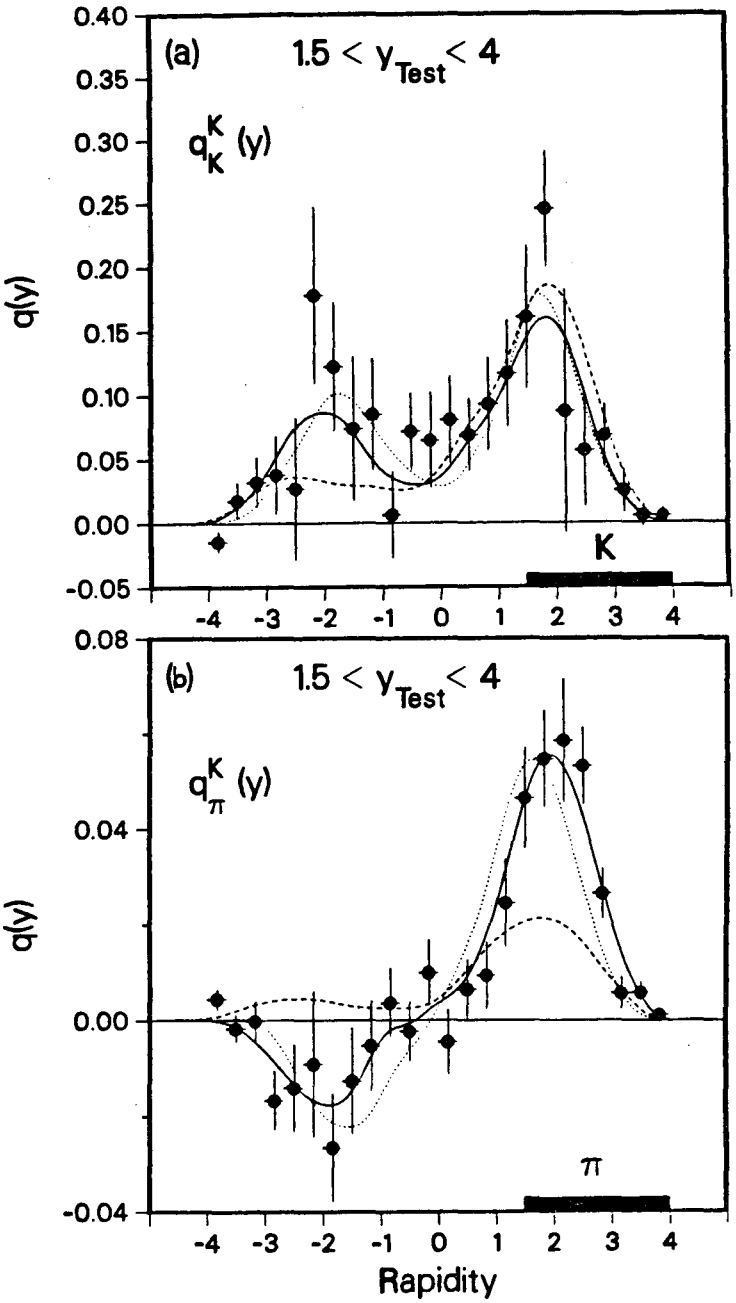

FIGURE 18

The KK associated charge density for large rapidities is shown in (a) and the πK associated charge density for the same rapidity interval is shown in (b). The solid and dotted lines show the predictions of the LUND and Webber models. The dashed line gives the predictions of the LUND model without heavy quarks. The data is from the TPC.

comparable in size to the SRC and large in contrast to the $\pi\pi$ case in which the LRC was a factor of six smaller than the SRC. Unlike the $\pi\pi$ case, the decay of resonances is expected to be a small contribution to the SRC. For small y_{test} the ϕ is expected to contribute about 10% of the SRC, and it should be the only contribution if primary mesons are produced in the ground state scalar and vector nonets. For large y_{test}, the ϕ contributes about 15% and the $F \longrightarrow \phi\pi$ contributes about 5% of the SRC. It appears, therefore, that the KK SRC cannot be explained by resonance decay and is evidence of soft hadronization with local compensation of flavor. The relatively large LRC shown in the figure indicates that for this y_{test} a large fraction of the K's are direct descendants from primary heavy quarks.

Figure 18b shows the size of the πK correlation to be much smaller than either the $\pi\pi$ or the KK correlations. The observed SRC is due to a combination of local charge conservation during hadronization and decays such as $K^{*o} \longrightarrow K^{+}\pi^{-}$. It is interesting to note that the LRC is of opposite sign than the KK LRC as is expected from the decay of primary charm particles (see Figure 16).

The curves superimposed on Figures 17 and 18 correspond to the LUND model (solid line), the Webber QCD cluster model (dotted line) and the LUND model without heavy (b and c) quarks (dashed line). The latter model is included to show explicitly the SRC's and LRC's introduced by heavy quark decays. In general both the LUND and the Webber models represent the features of the data quite well. The small existing disagreements are not known to be fundamental at this time.

The global conclusions from these correlations studies are: short range

correlations exist and support the hypothesis that quantum numbers are locally conserved during the hadronization process, and long range correlations provide evidence that jets are produced by flavor carrying quarks. Furthermore the detailed information now available provides additional constraints on models.

B. Baryon-baryon correlation

While the production of quark-antiquark pairs out of the vacuum is a natural feature of most models, the production of three-quark color singlet states as required for baryon formation is often an ad-hoc feature of the models. Even to test whether baryon pairs are produced close by in rapidity space, i.e. compensate baryon number locally, or are produced more or less randomly in rapidity space, i.e. conserve baryon number globally, is a difficult experimental question. Baryons are less common, and the efficiency for identifying them is usually low. Data is now becoming available on baryon-baryon correlations, albeit with relatively low statistics. TASSO[45] has reported data on pp and $p\bar{p}$ correlations at baryon momenta in the 1 to 5GeV/c range showing evidence for local baryon compensation. TPC[46] with a considerably larger number of $p\bar{p}$ events (179) at momenta below 1.5 GeV/c also favors local baryon number conservation with 107 events in which both baryons go in the same direction, and 72 events in which they go in opposite direction.

This summer, data on $\Lambda\bar{\Lambda}$ correlations have become available from the TPC[18] and the MkII.[15] In the TPC there are 14 events with a pair of lambdas :

Λ-$\bar{\Lambda}$ = 11 *background* 1.4±1.2,

Λ-Λ = 3 *background* 2.1±0.9, and

$\bar{\Lambda}$-$\bar{\Lambda}$ = 0 *background* 0.6±0.7

where the backgrounds have been calculated with a Monte Carlo simulation and the errors include both statistical and systematic errors. The above $\Lambda\bar{\Lambda}$ pair multiplicity corresponds to $0.042 \pm 0.017 \pm 0.014$ pairs per event. For the MkII there are a total of 35 pairs with the following breakdown:

$$\Lambda\text{-}\bar{\Lambda} = 27 \quad \textit{background} \simeq 3,$$
$$\Lambda\text{-}\Lambda = 3 \quad \textit{background} \simeq 2, \text{ and}$$
$$\bar{\Lambda}\text{-}\bar{\Lambda} = 5 \quad \textit{background} \simeq 2.$$

For $\Lambda\bar{\Lambda}$ pairs, Figure 19a shows the distribution of opening angles and the distribution of rapidity gap for the TPC data. Figure 19b shows the equivalent distributions for the MkII data. The dashed curve for the TPC is the LUND model simulation and the curve for the MkII is a QCD model simulation. While the distributions are not directly comparable due to different detector acceptances, there is clear evidence that the $\Lambda\Lambda$ pairs tend to be produced with small rapidity gap indicating local baryon compensation. The TPC data shows two events at large rapidity gap which are a 2 s.d. effect above the LUND model predictions and may indicate the coexistence of mechanisms which enhance long range $\Lambda\Lambda$ correlations. No equivalent effect is seen in the Mk II data.

To derive a sense of the strength of the $\Lambda\bar{\Lambda}$ correlation it is necessary to compare it to various models. Figure 20 shows the relation between the $\Lambda\bar{\Lambda}$ pair multiplicity and the Λ,$\bar{\Lambda}$ single particle multiplicity. The two shaded bands correspond to two extreme assumptions: the top band corresponds to the assumption that Λ and $\bar{\Lambda}$'s are always produced as $\Lambda\bar{\Lambda}$ pairs, i.e a maximum correlation, and the bottom band corresponds to the assumption that the flavor of the baryon (B) and the antibaryon ($\bar{B}$) of a B-$\bar{B}$ pair are completely uncorrelated,

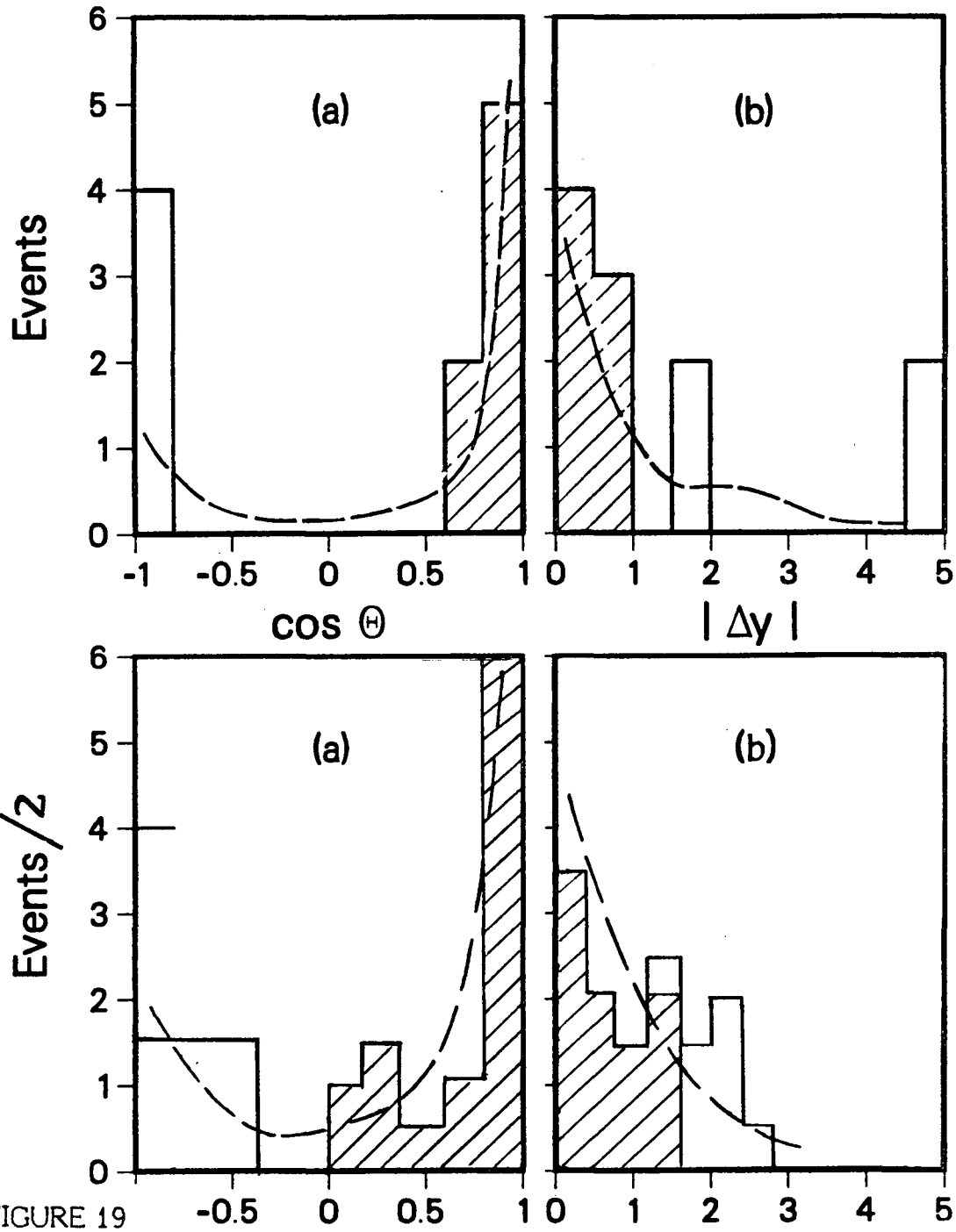

FIGURE 19

Distributions for the (a) opening angle between the Λ and $\overline{\Lambda}$ and (b) rapidity difference between the Λ and $\overline{\Lambda}$ for the TPC data (upper two plots) and the MKII data (lower two plots). The distributions have not been corrected for acceptance or backgrounds. The distributions are compared with model predictions.

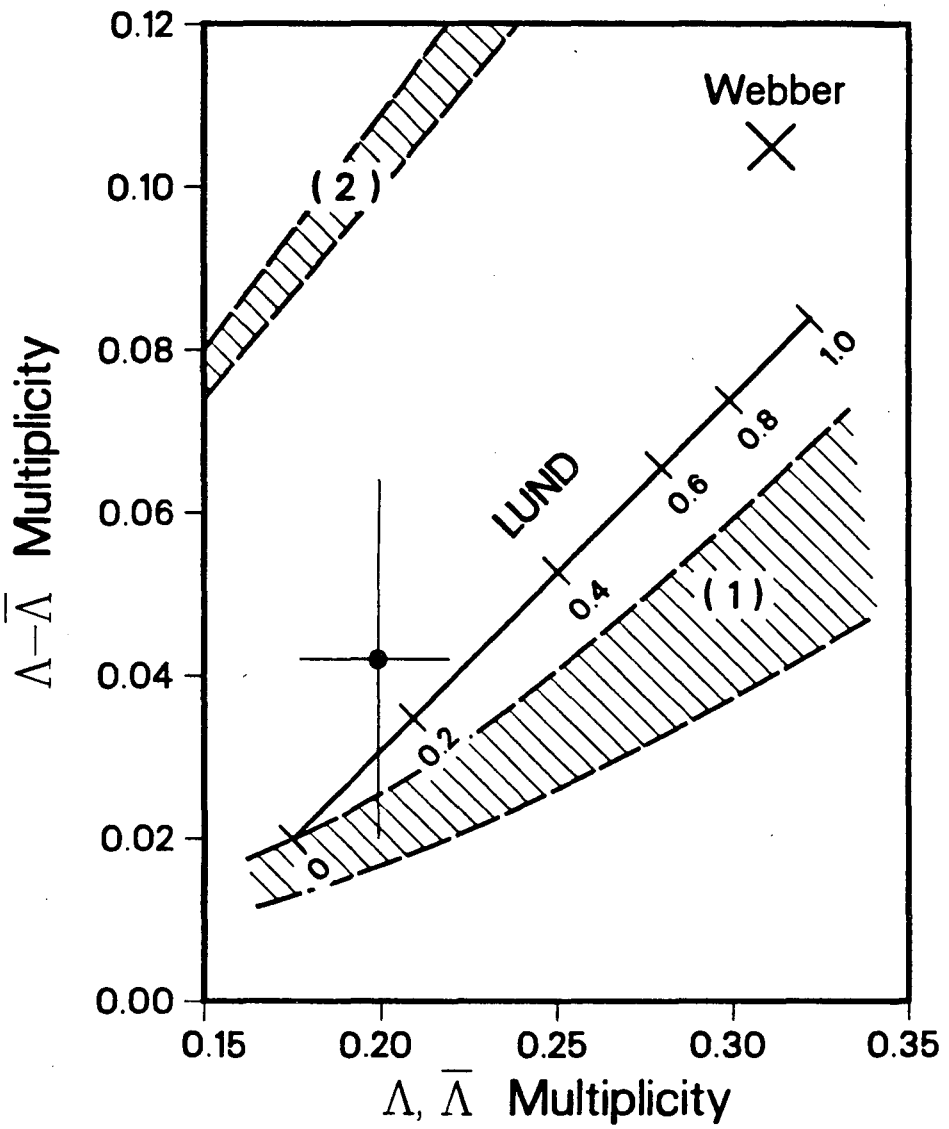

FIGURE 20

Λ, $\overline{\Lambda}$ multiplicity and Λ-$\overline{\Lambda}$ pair multiplicity for the TPC data (+) compared to the LUND (solid line) and the Webber model (x). The upper band corresponds to predictions in which the Λ and $\overline{\Lambda}$ are maximally correlated and the lower band to predictions in which the Λ and $\overline{\Lambda}$ are minimally correlated See text for details.

i.e a minimum correlation.. The bands are bands rather than lines because they include a range of assumptions on the multiplicity distribution of baryons per event. The data point lies much closer to the assumption of minimum correlation. Figure 20 also shows the result of two model calculations. The Webber model predicts higher multiplicities of both Λ's and $\Lambda\bar{\Lambda}$ pairs in disagreement with the data even though it predicts the right multiplicity for π, K and p. This model, however, was not optimized to fit the Λ distributions. The LUND model can give a range of values depending on the value of the extra suppression factor for strange diquarks, $(us/ud)/(s/d)$, where (s/d) is the production ratio of strange and ordinary quarks from the vacuum and (us/ud) is the production ratio for strange and ordinary diquarks. A value $(us/ud)/(s/d)$ of $\simeq .2$ is in reasonable agreement with the data. Thus strange diquarks are suppressed by an additional factor of five when compared to the suppression for single strange quarks in the LUND model.

The above studies are clearly limited by statistics and will slowly improve in time as detectors collect more statistics and PEP increases its luminosity.

V. CONCLUSIONS

From the above progress report it is clear that the subject is complex and that definitive tests of models are difficult. Small differences in predictions do count and can reflect real problems with models as was shown in the analysis of particle flow in three jet events. A large amount of new data has been added during the last year: there are new areas for models to try to fit and many cross checks for experimental results. A lot remains to be done, but there is hope if the progress of last year is a clue to the future.

REFERENCES

1. See M. Davier's review of PETRA results elsewhere in these proceedings.

2. See J. Chapman's review of heavy quark results from PEP elsewhere in these proceedings.

3. See for example J.Ellis, "*Jets in QCD: a Theorist's Perspective*", Proceedings of the 11th SLAC Summer Institute on Particle Physics, SLAC Report 267, July 1983.

4. G. Hanson et al., Phys. Rev. Lett. 35, 1609 (1975).

5. D.P. Barber et al.(MARK J), Phys. Rev. Lett. 43, 830 (1979); R. Brandelik et al.(TASSO), Phys. Lett. 86B, 243 (1979); Ch. Berger et al.(PLUTO), Phys. Lett 86B , 418 (1979); W. Bartel et al.(JADE), Phys. Lett. 91B, 142 (1980).

6. R.D. Field and R.P. Feynman, Phys. Rev. D15, 2590 (1977) and Nucl. Phys. B138, 1 (1978); P. Hoyer at al., Nucl. Phys. B161, 349 (1979); A. Ali et al., Phys.Lett. 93B, 155 (1980) and Nucl. Phys. B167, 454 (1980).

7. B. Andersson, G. Gustafson, G. Ingelman and T. Sjostrand, Phys. Reports 97, 31 (1983).

8. B. R. Webber, Nucl. Phys B238, 492 (1984).

9. T.D. Gottschalk, Nucl. Phys. B239, 325 (1984); B239, 349 (1984).

10. A compilation of model predictions for particle production is contained in L. Galtieri's review of "*Quark Fragmentation in e+e- Annihilation*", LBL-18424, to be published in the proceedings of the XV Symposium on Multiparticle Dynamics, Lund, Sweden, June 10-16, 1984.

11. M. Derrick et al., "*Study of Quark Fragmentation at High Z*", results submitted to the XXII International Conference on High Energy Physics, Leipzig, DDR, July 19-25, 1984.

12. G.R. Farrar and D.R. Jackson, Phys. Rev. Lett. 35, 1416 (1975); see also R.D. Field and R.P. Feynman, Nucl. Phys. B138, 1 (1978).

13. H. Aihara et al.(TPC), Phys. Rev. Lett. 52, 2201 (1984).

14. The HRS results on ϕ production have been presented by M. Derrick et al., "*Observation of F(1975)in e+e- Annihilation at 29 GeV*", submitted to the XXII International Conference on High Energy Physics, Leipzig, DDR, July 19-25, 1984.

15. V. Luth (MKII), informal report submitted to this conference for this presentation.

16. M. Althoff et al.(TASSO), Phys.Lett. 130B, 340 (1983)

17. W. Bartel et al.(JADE), Phys. Lett. 104B, 325 (1981)

18. H. Aihara et al.(TPC), "Λ *Production in e+e- Annihilation at 29 GeV*", LBL - 18382, submitted for publication, October 1984.

19. H. Aihara et al.(TPC), "K^{*o} *and* K^{o} *Meson Production in e+e- Annihilation at 29 GeV*", LBL-18325, submitted for publication, September 1984.

20. R. Brandelik et al. (TASSO), Phys. Lett. 117B, 135 (1982).

21. H. Aihara et al. (TPC), Phys. Rev. Lett. 52, 577 (1984).

22. H.M. Schellman (MKII), "*Measurement of Strange and Vector Particle Cross Sections*", informal report submitted to this conference for this presentation.

23. S. Ahlen et al. (HRS), "K^{o} *and* Λ *Production at Ecm = 29 GeV in the PEP High Resolution Spectrometer*", informal report submitted to this conference for this presentation.

24. W. Bartel et al. (JADE), "*Inclusive Production of Vector Mesons* ρ^{o} *and* $K^{*\pm}$ *in e+e- Annihilation at* $\sqrt{s}$ *= 35 GeV*", DESY 84-58 preprint, 1984.

25. DELCO Collaboration, preliminary results presented at the 1984 Vanderbilt conference on e+e- Collisions. See for example W. Hofmann, " *Hadron Production in e+e- Annihilation at PEP*", LBL-17845, May 1984.

26. H.M. Schellman (MkII), "$K^{\pm}$ *Cross Sections*", informal report submitted to this conference for this presentation.

27. M. Althoff et al. (TASSO), Z. Physik C17, 5 (1983).

28. R. Brandelik et. al. (TASSO), Phys. Lett. 94B, 91, (1980); see also S.L. Wu, Physics Reports vol.107, num. 2-5, May 1984.

29. W. Bartel et al. (JADE), Z. Physik C20, 187, (1983).

30. H. Aihara et al. (TPC), " *Inclusive* γ *and* π^{o} *Production Cross Section and Energy Fractions in e+e- Annihilation at 29 GeV*", submitted for publication October 1984.

31. R. Brandelik et al.(TASSO), Phys.Lett. 108B, 71 (1982). For the most comprehensive π^{0} measurement at PETRA see H.J. Behrend et al. (CELLO), Z. Physik C20, 207 (1983).

32. W. Bartel et al. (JADE), Phys. Lett. 130B, 454 (1983).

33. M.Derrick et al., "*Vector Meson Production in e+e- Annihilation at Ecm = 29 GeV in the High Resolution Spectrometer*", submitted to the XXII International Conference on High Energy Physics, Leipzig, DDR, July 19-25, 1984.

34. D. Blockus and B. Brabson, "*Comment About Our HRS rho/pi Ratio in e+e- Scattering*", informal comment submitted to this conference for this presentation.

35. R. Brandelik et al. (TASSO), Phys. Lett. 114B, 65 (1982); M. Althoff et al. (TASSO), Z. Physik. C22, 307 (1984).

36. H. Aihara et al. (TPC), Phys. Rev. Lett. 53, 130 (1984).

37. W. Bartel et al. (JADE), Phys. Lett. B134, 275, (1984) .

38. A. Petersen , "*Further Studies on Quark and Gluon Fragmentations. Recent Results from Jade*," to appear in the Proceedings of the XV Symposium on Multiparticle Dynamics, Lund, Sweden, June 10-16, 1984.

39. H.Aihara et al. (TPC), "*Tests of Models of Parton Fragmentation Using 3-jet Events in e+e- Annihilation at* $\sqrt{s}$ *= 29 GeV*", LBL-18407, submitted for publication, October 1984.

40. H. Aihara et al. (TPC), "*Tests of Models for Quark and Gluon Fragmentation at* $\sqrt{s}$ *= 29 GeV*", LBL-18408, submitted for publication, October 1984.

41. E. Fernandez et al., "*A Measurement of Energy-Energy Correlations in e+e- to Hadrons at* $\sqrt{s}$ *= 29 GeV*", submitted to the XII International Conference on High Energy Physics, Leipzig, DDR, July 19-25, 1984.

42. H. Aihara et al. (TPC), "*Observation of Strangeness Correlations in e+e- Annihilation at* $\sqrt{s}$ *= 29 GeV*", LBL-18125, submitted to Phys. Rev. Lett.

43. R Brandelik et al.(TASSO), Phys. Rev. Lett. 100B, 357 (1981); Ch. Berger et al. (PLUTO), Nucl. Phys. 214B, 189 (1983).

44. D. Drijard et al., Nucl. Phys. 166B, 233 (1980).

45. M. Althoff et. al. (TASSO), Phys. Lett. 139B, 126 (1984).

46. K. Maruyama (TPC), "*Baryon Production in e+e-Annihilation at Vs = 29 GeV*", U. of Tokyo preprint UT-HE-84/09, to appear in the Proceedings of the Hadronic Sessions of the Nineteenth Recontre de Moriond, edited by J. Tran Thanh Van.

TECHNICAL INFORMATION DEPARTMENT
LAWRENCE BERKELEY LABORATORY
UNIVERSITY OF CALIFORNIA
BERKELEY, CALIFORNIA 94720

O. Bauer
271-0102

8:15 8 4:30
10:20 10 9:45
D.S.S. 400 P.I.